Bioactive Materials 6 (2021) 3947–3961

Contents lists available at ScienceDirect

Bioactive Materials

journal homepage: www.sciencedirect.com/journal/bioactive-materials

Tuning gelatin-based hydrogel towards bioadhesive ocular tissue engineering applications

Sina Sharifi [a], Mohammad Mirazul Islam [a], Hannah Sharifi [a], Rakibul Islam [b], Darrell Koza [c], Felisa Reyes-Ortega [g], David Alba-Molina [g], Per H. Nilsson [b,d], Claes H. Dohlman [a], Tom Eirik Mollnes [b,e,f,h], James Chodosh [a], Miguel Gonzalez-Andrades [a,g,*]

[a] Massachusetts Eye and Ear and Schepens Eye Research Institute, Department of Ophthalmology, Harvard Medical School, Boston, MA, USA
[b] Department of Immunology, Oslo University Hospital, Rikshospitalet, University of Oslo, Oslo, Norway
[c] Department of Physical Sciences, Eastern Connecticut State University, Willimantic, CT, USA
[d] Linnaeus Center for Biomaterials Chemistry, Linnaeus University, Kalmar, Sweden
[e] Research Laboratory, Nordland Hospital, Bodø, Norway
[f] Centre of Molecular Inflammation Research, Norwegian University of Science and Technology, Trondheim, Norway
[g] Maimonides Biomedical Research Institute of Cordoba (IMIBIC), Department of Ophthalmology, Reina Sofia University Hospital and University of Cordoba, Cordoba, Spain
[h] Faculty of Health Sciences, K.G. Jebsen TREC, University of Tromsø, Norway

ARTICLE INFO

Keywords:
Natural-based hydrogel
Gelatin
Biocompatible
Biomimetic
Bioadhesive
Cornea

ABSTRACT

Gelatin based adhesives have been used in the last decades in different biomedical applications due to the excellent biocompatibility, easy processability, transparency, non-toxicity, and reasonable mechanical properties to mimic the extracellular matrix (ECM). Gelatin adhesives can be easily tuned to gain different viscoelastic and mechanical properties that facilitate its ocular application. We herein grafted glycidyl methacrylate on the gelatin backbone with a simple chemical modification of the precursor, utilizing epoxide ring-opening reactions and visible light-crosslinking. This chemical modification allows the obtaining of an elastic protein-based hydrogel (GELGYM) with excellent biomimetic properties, approaching those of the native tissue. GELGYM can be modulated to be stretched up to 4 times its initial length and withstand high tensile stresses up to 1.95 MPa with compressive strains as high as 80% compared to Gelatin-methacryloyl (GelMA), the most studied derivative of gelatin used as a bioadhesive. GELGYM is also highly biocompatible and supports cellular adhesion, proliferation, and migration in both 2 and 3-dimensional cell-cultures. These characteristics along with its super adhesion to biological tissues such as cornea, aorta, heart, muscle, kidney, liver, and spleen suggest widespread applications of this hydrogel in many biomedical areas such as transplantation, tissue adhesive, wound dressing, bioprinting, and drug and cell delivery.

1. Introduction

Hydrogels are three-dimensional (3D) networks of crosslinked polymers, engineered to structurally and biologically support cellular growth, migration, and tissue formation [1,2]. Although their biomimetic behaviors including biocompatibility [3], biodegradation [4], and responsiveness to an external stimulus [5] can be controlled, their relatively low mechanical and adhesion characteristics pose crucial challenges, obstructing their translation into clinical medicine.

Multicomponent interpenetration polymer networks (mIPNs) [6–8], macromolecular microsphere composites (MMC) [9], nanocomposite physical hydrogels [10], double crosslinked polymeric networks [11], tetrahedron-like structures with homogeneous spacers [12], slide-ring connected materials [13], and dynamically crosslinked systems [14,15] are among the approaches to enhance the mechanical properties of hydrogels. These approaches often require the incorporation of synthetic materials such as polyacrylic acid (PAA) [6,8], polyacrylamide [7,11], poly-ethylene glycol (PEG), PAA/polystyrene/poly butyl acrylate [9], hybrid silica nano-particles (VSNPs)/PAA [10], Tetrahydroxyl-Terminated PEG [12], Polyrotaxane (PR) [13], and

Peer review under responsibility of KeAi Communications Co., Ltd.
* Corresponding author. 20 Staniford St, Boston, MA, 02114, USA.
E-mail addresses: Miguel_gonzalez@meei.harvard.edu, miguel.gonzalez@imibic.org (M. Gonzalez-Andrades).

https://doi.org/10.1016/j.bioactmat.2021.03.042
Received 29 January 2021; Received in revised form 26 March 2021; Accepted 26 March 2021

stearyl methacrylate (C18)/dodecyl acrylate copolymer [14] along with carboxyl-functionalized polystyrene [15] into natural-based hydrogels matrices, involving covalent and non-covalent (i.e. electrostatic forces, hydrophobic interactions, hydrogen bonding, van der Waals forces) or combinations of these interactions in reinforcement process [6].

However, such incorporation may alter the chemical composition of the hydrogel and adversely impact their biological properties. On the other hand, many biomedical applications of hydrogels, including tissue repair [16], drug delivery [17], wound dressings [18], and biomedical devices [19] require strong adhesion between the hydrogel and the dynamic surface of the host tissue. Thus, the incorporation of such adhesion properties into the hydrogel structure is crucial and can significantly facilitate hydrogel translation into clinical medicine [20].

One of the most widely used biomaterials for hydrogel manufacturing, because of its cheapness and high-biocompatibility, is gelatin and its derivatives. Gelatin is a polydisperse protein produced from irreversible hydrolysis of collagen fibrils into lower molecular weight polypeptides. Although the chemical composition of gelatin is similar to those of the parent collagen, it possesses better solubility and lesser antigenicity [21,22]. These render gelatin as an excellent component for stimulating cellular attachment and growth, including the possibility of regulating matrix metalloproteinase degradation. Despite the development of various crosslinking strategies to generate gelatin-based hydrogels [23–26], adequate mechanical and adhesion characteristics have yet to be realized. For instance, gelatin methacryloyl (GelMA), the most studied derivative of gelatin [27], demonstrated maximum elastic modulus and ultimate tensile strength 180 ± 34, 53 ± 17 KPa, respectively [28], which are almost 2 orders of magnitude lower than those reported for the human cornea (i.e. 15.86 ± 1.95 and 3.29 ± 1.95 MPa, respectively) [29]. A recent modification in the crosslinking of GelMA was reported to increase the elastic modulus and tensile strength up to 224.4 ± 32.3 and 45.3 ± 4.1 KPa, respectively [30], yet fall short of those reported for human tissues.

It has been shown that enhancing the degree of methacrylation or FD significantly enhances the mechanical properties of the resulting hydrogel [27,31]. However, the methacrylation degree of gelatin has been constrained by the low abundance of nucleophilic amino acids (mostly primary amine bearing amino acids such as lysine and hydroxylysine), which can undergo a single methacrylation reaction to form amide bond [27]. To extend the functionalization degree to a wider range, we functionalized gelatin with glycidyl methacrylate that undergoes epoxide ring-opening reaction and forms a secondary amine that can also react with another glycidyl methacrylate (Fig. 1a), generating the precursor of Gelatin-glycidyl-methacrylate hydrogel (abbreviated or called as GELGYM). This GELGYM precursor potentially hold twice the methacrylate groups compared to GelMA (two glycidyl methacrylate per each amine bearing amino acid).

GELGYM precursor generates a hydrogel after crosslinking under low-intensity visible light. This simple modification of GelMA formed from grafting functional crosslinkable moieties onto a gelatin backbone facilitates the tuning of the mechanical and adhesive properties of gelatin scaffolds. To validate that hypothesis, GELGYM was tuned based on functional degree, precursor concentration, and crosslinking time, to optimize its corneal application. The corneal model was used because of its high optical and mechanical requirements, in addition to the complexity of combining different cell populations. Finally, we obtained robust biomaterials and strong adhesion to biological tissues, in addition to maintaining the highly biocompatible nature of the hydrogel to support cellular adhesion, growth, and migration. The tuning of gelatin-based hydrogels described here might benefit various fields of biomedical engineering and regenerative medicine including ophthalmology.

2. Materials and methods

2.1. Materials

All chemicals were used as received from Sigma-Aldrich (St. Louis, MO) without further modification unless otherwise noted. Human donated corneas were kindly provided by VisionGift (Boston, MA) for research purposes only. Each donated cornea was obtained from

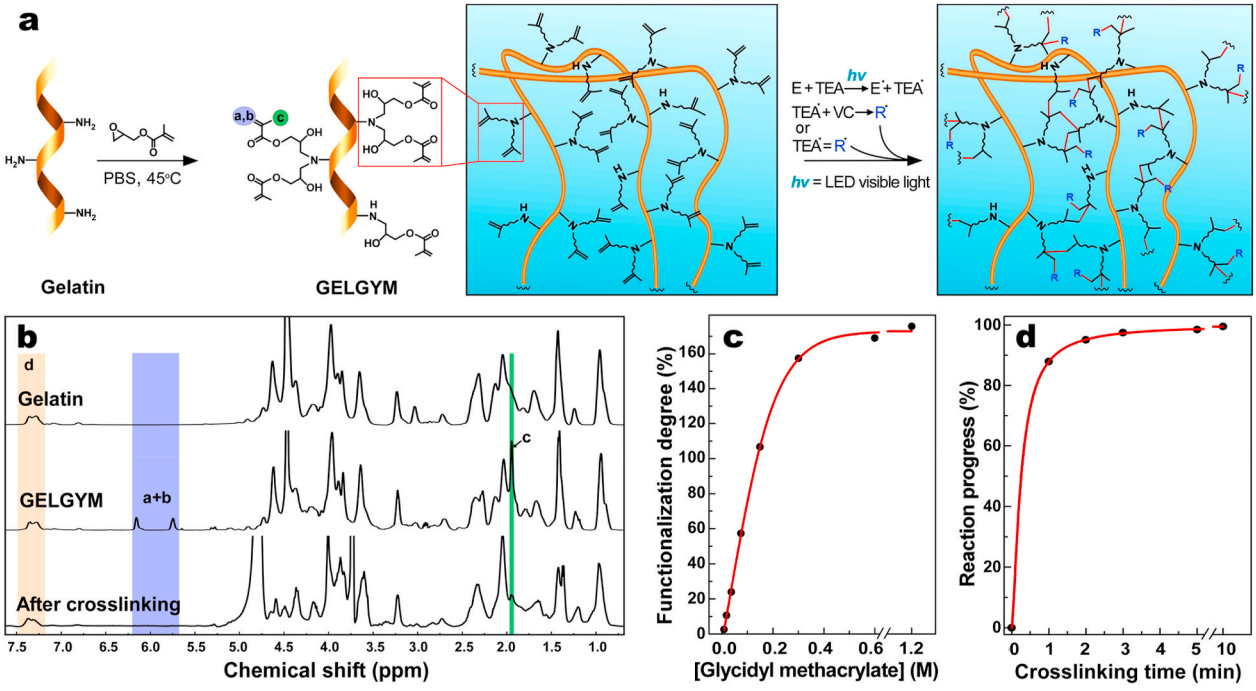

Fig. 1. Synthesis, and chemical characterization of GELGYM. a) Schematic of chemical synthesis of GELGYM via epoxide ring-opening reaction of glycidyl methacrylate with gelatin and its crosslinking with a visible LED in the presence of E (0.05 mM), TEA 0.04%, and VC (0.04%) to form a 3-dimensional network of the hydrogel. b) ^{1}H-NMR characterization of the GELGYM before and after crosslinking. c) FD tunability of GELGYM through varying the concentration of glycidyl methacrylate in the reaction, and d) crosslinking progress dependence on the crosslinking time (CT), characterized by ^{1}H-NMR.

cadaveric donors and processed in eye, organ, or tissue banks where the donated cornea was de-identified. Massachusetts Eye and Ear does not require Ethical Committee approval for the use of this type of human samples. Human blood drawn from healthy donors was used in complement activation experiments. This part of the study was performed with the consent of the local ethical committee at Oslo University Hospital, Norway.

2.2. Chemical synthesis of GELGYM

To synthesize GELGYM with different functionalization degree (FD), a gelatin solution (10 g/mL) (porcine skin origin, 300 g Bloom, type A) prepared in PBS was mixed with different amounts of glycidyl methacrylate (GMA) (0.0125, 0.025, 0.05, 0.1, 0.2, 0.4, 0.8, 1.6 mL) and added to the respective vials to form reaction solutions with varying concentrations of GMA (from 9.5 mM to 1.2 M). The reaction mixtures were agitated for 4 h at 45 °C, diluted with deionized water (10 mL), and then dialyzed for 1 week using dialysis membrane with molecular weight cut-off of 14 kDa (Sigma-Aldrich) to make sure that unreacted glycidyl methacrylate was washed out. Finally, they were freeze-dried for 3 days to obtain foam-like GELGYM precursors with different FDs.

2.3. Chemical synthesis of GELMA

To synthesize GelMA with a high FD, a gelatin solution (10 g/mL) (porcine skin origin, 300 g Bloom, type A) was dissolved in PBS, followed by the addition of methacrylate anhydride (8 mL, 0.05 M) as described elsewhere [30]. The reaction mixtures were agitated for 3 h at 50 °C, diluted with deionized water (10 mL), and then dialyzed for 1 week using dialysis membrane with molecular weight cut-off of 14 kDa (Sigma-Aldrich) at 50 °C. Afterward, the GelMA solution was freeze-dried for 3 days to obtain foam-like GelMA.

2.4. Crosslinking conditions

To prepare GELGYM solutions with different precursor concentrations, PBS (2.45 mL) was added to varying amounts of GELGYM (0.334, 0.445, 0.667, 0.890, and 1.00 g) and stirred at 45 °C to generate a homogenous solution. The solution was mixed with the crosslinking solution (1 mL) containing eosin Y (0.22 mM), triethanolamine (1.78% w/v), and vinyl caprolactam (VC) (1.78% w/v) in the dark, where eosin Y acted as a photoinitiator, triethanolamine (TEA) as an electron donor, and N-vinyl-caprolactam as an accelerator [32] (Fig. S1). Visible light crosslinking eliminates the potential side effects of UV crosslinking. Afterward, the resulting prepolymer solution was carefully transferred to an appropriate mold or applied to the desired structure and crosslinked for varying times (1, 2, 3, 5, and 10 min) using our hand-made visible light source (LED with a wavelength range of 505–515 nm and the intensity of 20 mW/cm^2). In the case of GelMA, the precursor (0.890 g) was added to PBS (2.45 mL), stirred at 45 °C, and mixed with the same crosslinking solution (1 mL) as explained above to generate GelMA solution (20% w/v). We used the same light source to crosslink the GelMA.

2.5. Chemical characterization (^{1}H-NMR)

All ^{1}H-NMR experiments were performed on 400-MHz NMR (JEOL; Peabody, MA) and chemical shifts reported relative to 3-(trimethylsilyl)-propionic-2,2,3,3-d4-acid as the internal standard. A small amount of GELGYM (10 mg) mixed with D_2O (0.5 mL) in an NMR tube was heated for 30 min at 40 °C to fully dissolve the precursor and the spectra were recorded while the sample was maintained at 30 °C. For crosslinked samples, the prepolymer solution (80 μL) was transferred to a cylindrical mold (0.6 mm diameter, and 0.2 mm depth), crosslinked, and washed with water. Afterward, the samples were incubated in collagenase solution (2 mL, 10 U/ml), containing Tris-HCl buffer (0.1 M) with a pH of 7.4 supplemented with $CaCl_2$ (5 mM) at 37 °C to digest the hydrogel and form a homogenous solution. Then, the solutions were freeze-dried to eliminate the water and similar to non-crosslinked samples were dissolved in D_2O at 30 °C and their ^{1}H-NMR spectra were acquired.

2.6. Mechanical characterization

Hydrogels with varying FD, crosslinked for varying periods of time (1–10 min) were prepared as described above. Mechanical testing (tensile and compression) was conducted using a mechanical tester (Mark-10 ESM 303; Copiague, NY). For tensile tests, dumbbell-shaped hydrogels (total length of 15 mm, a gage area of 3 × 1 mm^2, grip area 6 × 4 mm^2 and thickness of 1 mm) were fastened to the mechanical tester grips and stretched at a rate of 2 mm/min until rupture. The stress was recorded as a function of the strain. The obtained stress/strain curve was used to extract elastic modulus, ultimate tensile strength, elongation, and energy at break for each specimen [n = 8].

The elastic modulus was determined from the linear derivatives of the stress/strain plot at 0–60% strain. The energy at break was calculated from area under curve of stress/strain plot at 0–100% strain. For compression tests, cylindrical samples (diameter (d) = 0.7 mm, and thickness (th) = 0.2 mm) were placed in a mechanical tester and testing was performed with the crosshead speed of 0.5 mm/min until the maximum stress of 0.6 MPa. The compressive stress was recorded as a function of the strain. The obtained stress/strain curve was used to extract the compressive modulus of each specimen [n = 8].

2.7. Swelling ratio

To measure the swelling ratio, first, we made disc-shape constructs (d = 7 mm and th = 2 mm). These were washed with water and blot dried to obtain their initial weights (Wi) before their immersion in PBS solution and incubated at 37 °C. After predetermined periods of time (1–4 days), swollen hydrogel samples were rinsed with water, their surface water was removed, and swollen weights (Ws) were measured. The swelling ratio (S) for the hydrogels [n = 5] was obtained according to the following equation:

$$S(\%) = \frac{(W_s - W_i)}{W_i} \times 100$$

2.8. Glucose diffusion

Designing hydrogel formulations for tissue engineering applications requires knowledge of its diffusion permeability, especially to glucose, to ensure the correct nutrition of the scaffold and its biointegration into the host tissue. Therefore, a study to determine the permeability coefficients of GELGYM for different glucose concentrations was carried out. A Static Franz cell system composed of 1-mL upper cell cap and a 5-mL lower receptor chamber with a diameter of 9 mm (PermeGear; Hellertown, PA) was used to measure the permeability of GELGYM hydrogels and corneal samples as controls (Section B of SI). First, GELGYM solution (200 μL) was prepared and transferred to a PDMS mold (d = 15 mm and th = 0.8 mm), crosslinked for varying periods of time (1–10 min), and washed with water to form disc-shaped GELGYM constructs. The constructs and 15-mm diameter discs of trephined fresh porcine corneas (Pel-Freez Biologicals, Rogers, AR) as controls were each inserted between the two compartments of Franz cell, creating a barrier between the two chambers. The upper section was filled with PBS (1 mL) and the bottom part was filled with glucose solution (5 mL, 1000 mg/dL). Both chambers were equipped with a small stirrer bar, and the solutions were mixed with a magnetic stirrer throughout the experiment, and the entire unit was placed inside of an incubator at 37 °C. After glucose had diffused through the membrane for different time points, the glucose concentration in the upper chamber was measured using a Counter Next EZ blood glucometer (Bayer; Parsippany, NJ) with glucose test strips [n = 4].

2.9. Optical transmission

The optical transmissions of GELGYM hydrogels and those of human corneas were examined by a UV–Vis spectrometer (Molecular Devices SpectraMax 384 Plus Microplate Reader, Molecular Devices; San Jose, CA). First, the GELGYM solution (40 μL) was transferred to a PDMS mold (d = 6 mm and th = 1 mm) and crosslinked for varying times (1–10 min) to yield disc-shaped constructs. The constructs and 6-mm diameter trephined discs of fresh human corneas (controls) were placed in individual wells of a 96-well quartz microplate, filled with water, and their optical transmittance was recorded from 250 to 850 nm in quartz microplate at 1-nm wavelength increments. The transmittance of the samples [n = 4] was corrected with blank media (distilled and filtered water) and the mean transmittance (%) for each group calculated and plotted as a function of wavelength.

2.10. In vitro biodegradation

Enzymatic degradation of GELGYM hydrogels was evaluated using collagenase from Clostridium histolyticum, as reported elsewhere [33,34]. Briefly, the GELGYM solution (80 μL) was transferred to a PDMS mold (d = 6 mm and th = 2 mm) and crosslinked for varying times (1–10 min) to yield disc-shaped constructs. Then, the discs were washed with water, lyophilized, and weighed to obtain their dried weight (Wi). Afterward, they were soaked in PBS for 1 h to reabsorb the water, and along with 6-mm trephined fresh porcine corneas as a control, were placed in a solution containing collagenase (5 U/mL) in Tris-HCl buffer (0.1 M, pH of 7.4), supplemented with $CaCl_2$ (5 mM) and incubated at 37 °C. The collagenase solution was changed every 8 h and the residue was carefully removed from the solution, rinsed with water and lyophilized, and its dried mass at different time points (Wf) was weighed. The degradation rate was calculated [n = 4] using the following equation:

$$Lost\ Weight\ (\%) = 100 - \frac{W_f - W_i}{W_i} \times 100$$

2.11. In vitro and ex vivo biocompatibility

2.11.1. Live-dead assay

To evaluate the interaction of human corneal epithelial cells (HCEp), corneal fibroblasts (HCF) and corneal endothelial cells (HCEn), and hybrid neuroblastoma cells (NDC) with the GELGYM surface, we performed a standard Live-Dead assay as described elsewhere [35,36]. Briefly, the GELGYM solution (40 μL) was transferred to a PDMS mold (d = 15 mm and th = 1 mm), crosslinked for varying times (3, 5, and 10 min), washed with water, and immersed in PBS overnight. Samples were trephined with a 6-mm biopsy punch to generate 6-mm "culture discs" which then were transferred to individual wells of a 96-well plate. Before performing the in vitro study and seeding cells, those culture discs were sterilized with 3X antibiotic solution consisting of 300 unit/mL penicillin and 300 μg/mL streptomycin as previously described [37]. Then, HCEp, HCF, HCEn, or NDC (10,000) were seeded on each disc, followed by the addition of appropriate media [38] (100 μL) and incubated at 37 °C in 5% CO_2. Cell culture media was changed every 3 days. After 6 days of incubation, Live-Dead staining was performed on the cultured discs using a commercial kit (LIVE/DEAD™ viability/cytotoxicity kit, for mammalian cells, Thermofisher Scientific; Cambridge, MA), where cells were double-stained with calceinacetoxymethyl and ethidium homodimer. For Live-Dead study, calceinacetoxymethyl and ethidium homodimer was diluted in the cell culture media with the dilution of (1:1000), and (4:1000), respectively, which then was added to cells cultured on the discs and incubated at 37 °C for 30 min. Then, those cells were imaged by inverted fluorescent microscopy (Zeiss Axio Observer Z1; Thornwood, NY) with a 10× objective. Four samples for each group were tested and compared to the tissue culture well plate (TCP) as a control group.

2.11.2. 3D cell culture

To evaluate the interaction of human corneal fibroblasts (HCF) with the GELGYM in 3D cell culture, we 3D cultured HCF for 30 days and performed a standard Live-Dead assay. Briefly, the GELGYM (0.5 g) was incubated and dissolved in cell culture media (5 mL) at 37 °C overnight. Then, GELGYM solution was UV irradiated for 2 min using UV light transilluminator (TWM-20 transilluminator; Upland, CA) to sterilize the sample. Afterward, the solution was mixed with the crosslinking solution (1 mL) containing eosin Y (0.22 mM), triethanolamine (1.78% w/v), and vinyl caprolactam (VC) (1.78% w/v) in the dark. Afterward, the GELGYM solution was mixed with HCF suspended in cell culture media to afford 200,000 cells/1 mL solution, before transferring it into a PDMS mold (d = 6 mm and th = 1 mm) and crosslinked for varying times (3, 5, and 10 min). The samples were immediately immersed in cell culture media and incubated for 15 min, before transferring them to individual wells of a 24-well plate containing the cell culture media (1 mL). Cell culture media was changed every 2 days. After 1, 7, 14, and 28 days of incubation, Live-Dead staining was performed on the cultured discs using a commercial kit (LIVE/DEAD™ viability/cytotoxicity kit, for mammalian cells, Thermofisher Scientific; Cambridge, MA), where cells were double-stained with calceinacetoxymethyl (1:1000) and ethidium homodimer (4:1000), and incubated at 37 37 °C for 30 min. The discs were then imaged by confocal microscopy (Leica TCS-SP5 Upright Confocal Laser-Scanning Microscope; Buffalo Grove, IL) on an area of 1 × 1 mm^2 with depth of 0.5 mm in 100 frames.

2.11.3. AlamarBlue assay

To assess the metabolic activity of the cells cultured on the GELGYM discs, we used a standard AlamarBlue assay as described elsewhere [39]. Briefly, HCEp, HCF, HCEn, and NDC (10,000 per each well) were seeded on GELGYM culture discs with varying crosslinking times (CT) (3, 5, and 10 min), followed by the addition of appropriate media (100 μL), as previously described, and incubated at 37 °C and 5% CO_2. The AlamarBlue study was performed on day 2, day 4, and day 6 after cell seeding. At each time point, the tissue culture media was removed and replaced with fresh media (100 μL) containing resazurin sodium salt (0.004% w/v) and incubated for 2 h. Afterward, the media (95 μL) was removed from each well and pipetted into a new 96 well plate and read on a BioTek plate reader (Synergy 2, BioTek Instruments; Winooski, VT) at 530/25 nm for excitation and 600/25 nm for emission, and corrected with the fluorescence of GELGYM discs incubated without cells. Four samples for each group and 3-time points were tested and compared to tissue culture well plates as a control group (corrected with TCP without cells) and reported as mean ± standard deviation.

2.11.4. Ex vivo retention test

To evaluate the retention of the GELGYM, human corneoscleral limbus from several cadaveric donors were each sliced into 16 pieces (1 × 3 mm). Afterward, the GELGYM solution (FD of 175% and 22.5% w/v) was applied at the intersection of two fragments and crosslinked for 5 min. Then, those glued fragments were incubated under culture conditions in the appropriate media [DMEM/Ham's F-12 media, supplemented with newborn calf serum (10%), and EGF (10 ng/mL)] for 6 months (end of the experiment), and the retention rate was extracted from the number of constructs retaining their bonding compared to the beginning of the experiment.

2.11.5. Transmission electron microscopy (TEM)

After 1 and 6 months, the glued fragments from the retention test were removed from media, fixed in paraformaldehyde (4%), and then also fixed with half-strength Karnovsky's fixative (pH 7.4) (Electron Microscopy Sciences; Hatfield, PA), before placing them in fresh Karnovsky's fixative for 4 h. Afterward, the samples were washed (with three repeats) with Cacodylate Buffer (0.1 M) (Electron Microscopy Sciences) for 5 min and then rinsed with PBS. The specimens were post-fixed with osmium tetroxide (2%) (Electron Microscopy Sciences) for

1.5 h and stained with en bloc in aqueous uranyl acetate (2%) for 30 min. Afterward, the samples were dehydrated in ethanol and embedded in epoxy resin (Tousimis; Rockville, MD). Ultrathin sections (80 nm) were cut from each sample-block using a Leica EM UC7 ultramicrotome (Leica Microsystems; Buffalo Grove, IL) with a diamond knife, and mounted on grids. The thin sections on grids were stained with aqueous gadolinium (III) acetate hydrate (2.5%) and Sato's lead citrate stains using a modified Hiraoka grid staining system [40]. Sections were imaged by TEM with accelerating voltage at 80 kV (FEI Tecnai G2 Spirit TEM; Hillsboro, OR).

2.11.6. Immunohistochemistry (IHC)

The expression of specific markers by different cells that had migrated on the glued area from the retention experiment was determined by fluorescence immunohistochemistry on the paraffin-embedded tissue sections. First, paraffin was removed by xylene, and then, the samples were rehydrated in water through a graded series of alcohols (100%, 96%, 70%, 50%, and water). Next, tissue sections were incubated in sodium citrate buffer (10 mM), Tween 20 (0.05% w/w, pH 6.0) at 60 °C for overnight, and washed with tris-buffered saline (TBS) and Triton X-100 (0.025% w/w), followed by blocking any unspecific binding sites using TBS supplemented with fetal bovine serum (FBS) (10%) and bovine serum albumin (BSA) (1%). The sections were then incubated with the corresponding primary antibodies, as listed below, overnight at 4 °C in humidifying conditions: (i) Mouse monoclonal antibodies against HCEp specific cytokeratin (*anti*-cytokeratin 3 + 12, clone AE5; ab68260, dilution 1:50, abcam [Cambridge, MA]); (ii) mouse monoclonal antibody against ALDH3A1 (clone 1B6; GTX84889, dilution 1:50, GenTex [Zeeland, MI]); (iii) mouse monoclonal antibodies against alpha smooth muscle actin (clone 1A4; ab781, dilution 0.5 μg/mL, abcam). Then, the specimens were incubated with FITC-conjugated anti-mouse antibody (ab6785, dilution 1:100, abcam) as a secondary antibody for 1 h at room temperature. Finally, the slides were mounted in VectaShield mounting media containing DAPI (Vector Laboratories, Burlingame, CA), and imaged by an inverted fluorescent microscope (Axio Observer Z1, Zeiss).

2.11.7. Immunocytochemistry (ICC)

To evaluate the expression of ZO-1 marker by HCEn cultured on GELGYM, we used standard ICC assay. Briefly, HCEn (10000 cells per well) were seeded on GELGYM culture discs with varying CT (3, 5, and 10 min). At confluency, the discs were removed from media, carefully rinsed with PBS, and fixed in paraformaldehyde (4%). For permeabilization and blocking, discs were incubated in PBS containing Triton X-100 (0.25%) for 10 min and FBS (5%) in PBS containing Tween-20 (0.05%) for 1 h, respectively. The discs were then incubated with the rabbit polyclonal antibody against ZO-1 (ZO-1 Polyclonal Antibody, dilution: 1:100, ThermoFisher Scientific) as a primary antibody overnight at 4 °C in humidifying condition. Afterward, the specimens were incubated with Cy5-conjugated anti-Rabbit antibody (dilution: 1:200, abcam) as a secondary antibody for 1 h at room temperature. Samples were stained with DAPI (Vector Laboratories) for nuclear staining. Images were taken by a fluorescent microscope (Axio Observer Z1, Zeiss).

2.11.8. Ex vivo complement activation experiments

Human blood was drawn from healthy donors into Vacutainer™ tubes (Becton, Dickinson, and Co., Plymouth, UK) containing a specific thrombin inhibitor, lepirudin (Refludan®, Aventis Pharma [Mumbai, India]) at a final concentration of 50 μg/mL [41]. For each set of experiments, 300 μL of the blood was aliquoted into each 1.8-mL round-bottom sterile polypropylene cryogenic vial (Nunc, Thermofisher Scientific) and incubated at 37 °C with two pieces of 6 mm diameter size GELGYM. Additional aliquots were used to measure the initial activation (T0) before starting the incubation and background activations (T30) without GELGYM under the same conditions. After the incubation, EDTA at 10 mM final concentration was added to all tubes to stop further complement activation. Plasma was collected after 30 min of incubation. The collected plasma was preserved at −70 °C. Complement activation was assessed by measuring soluble C3bc fragments, and the soluble terminal complement complex (sC5b-9) using ELISA as described previously [38,42–44]. Briefly, the assays were based on monoclonal antibodies detecting neo-epitopes exposed after activation hence, specifically measuring only components formed upon activation. C3bc was determined by sandwich ELISA, using mAb bH6 for capture, biotinylated polyclonal *anti*-C3, and HRP-conjugated streptavidin (GE Healthcare; Chicago, IL) for detection. sC5b-9 was determined using the *anti*-neo C9 monoclonal antibody aE11 (produced in our laboratory) for capture, and biotinylated monoclonal *anti*-C6 (clone 9C4, produced in our laboratory), and finally streptavidin-HRP conjugate was added for detection.

2.12. Ex vivo burst pressure test

To measure the adhesion strength and sealing properties of the GELGYM to biological tissue we used an adopted burst pressure test based on the ASTM F2392-04 standard (fresh porcine cornea was used instead of collagen sheet) [n = 6]. Fresh porcine eyes were obtained from adult pigs immediately after their death at a local slaughterhouse and inspected carefully to discard those showing any corneal damage. Selected corneas were removed from porcine eyes with a 16-mm diameter trephine and washed with PBS. Then, the corneas were full-thickness trephined at varying sizes (2–8 mm), and placed in an artificial corneal chamber (Barron Precision Instruments; Grand Blanc, MI) equipped with a syringe pump (NE-300, ArrEssPro Scientific; Farmingdale, NY), loaded with PBS. The syringe was primed to fill the artificial chamber with PBS, and then the GELGYM solution (20–50 μL depending on the size of the defect) was applied into the defect using a micropipette and crosslinked by irradiation of LED light for varying CT (3–10 min). In case of larger perforations (≥6 mm), the first 20 μL of GELGYM solution was applied into the periphery of the either pre-crosslinked GELGYM patch, or corneal graft and then inserted in the perforated area. Immediately afterward, LED light for 0.5 min was applied to crosslink GELGYM and seal the perforation. Then, 50 μL of GELGYM solution was carefully applied onto the area and radiated for varying CT to completely seal the wound. The syringe was set to pump PBS (0.2 mL/min) into the chamber. The burst pressure was measured with a pressure sensor (PS-2017, PASCO; Roseville, CA) and recorded by computer via the PASCO Capstone interface.

Then, using PDMS mold, we generated a blood vessel-like tube with a length of 40 mm, an internal diameter of 5 mm, and thickness of 1 mm (5 min crosslinking). Then, the engineered tube was blocked from one end, and attached to a 7-mm plastic Hose Barb and secured with a rubber band (as shown in Supplementary Movie S5). The plastic valve was connected to the pressure sensor and the syringe pump. The syringe was filled with PBS, containing a blue dye for better visualization, and set to pump (0.2 mL/min) the solution into the engineered valve. The burst pressure was measured with a pressure sensor, recorded by a computer, and filmed by a Dino Lite camera (AM73915MZTL; Torrance, CA).

2.13. Lap shear adhesion test

The adhesion of GELGYM to various organs of lamb including aorta, muscle, heart, kidney, liver, and spleen (obtained from a local slaughterhouse) [n = 8] was evaluated according to modified ASTM F2255-05 standard lap shear test. Two polymethyl methacrylate (PMMA) slides (10 × 40 × 1 mm) were used to hold the tissue after functionalizing their surface. First, a glass coverslip (10 mm diameter) was functionalized with 3-(trimethoxysilyl)propyl methacrylate as previously described [45], then they were stuck with cyanoacrylate (Superglue Loctite, Henkel; Düsseldorf, Germany) to PMMA slide, and dried overnight (top slide). Then, using a blade, fresh tissue was dissected into 10 × 10 × 5 mm fragments and superglued on another PMMA slide (bottom one) and

air-dried for 1 min. Then, the prepolymer solution (50 μL) was added to the tissue and the other slide was carefully placed on the GELGYM solution. After assembly, the glue between the two slides was radiated to attach the tissue to the functionalized glass. The two PMMA slides were placed in the mechanical tester, and the shear test was run with 2 mm/min crosshead speed. The adhesive strength was measured at the point of detachment of the glue from the tissue. To compare the adhesion strength of GELGYM with traditional sutures (2-0, 4-0, and 9-0 Prolene sutures –Ethicon; Bridgewater, NJ-), we performed an ultimate tensile strength test. Briefly, we cut the suture into 10 cm sections and placed in the mechanical tester grips, and the ultimate tensile test was performed with 2 mm/min crosshead speed until the suture broke [n = 4].

2.14. Statistical analysis

One-way ANOVA with Tukey post hoc was used to compare burst pressure and metabolic activity between different groups. A value of $P < 0.05$ was considered statistically significant. ns, *, **, ***, and **** represent $p > 0.05$, $p < 0.05$, $p < 0.01$, $p < 0.001$ and $p < 0.0001$, respectively. GraphPad Prism 8.0 Software (GraphPad Software; CA) was used to analyze the data.

3. Results and discussion

3.1. Chemical synthesis and characterization

Gelatin-based hydrogels, and in particular, Gelatin methacryloyl (GelMA) have been extensively studied for biomedical applications, due to its excellent chemical and biological activities to promote cellular attachment and growth and ease of processing [23–27,31–46]. The influence of three different parameters has been studied in the preparation of gelatin-based hydrogels: precursor concentration ([GELGYM]), functionalization degree (FD), and crosslinking time (CT) (Table 1, Supplementary Information).

The FD was controlled through varying the amount of glycidyl methacrylate reactant added into the reaction mixture, ranging from 2.6% to 175% (on average per each amine bearing amino acid 1.75 glycidyl methacrylate attached) as shown in Fig. 1a–c and Supplementary Fig. S3. The characterization and quantification of the FD of GELGYM were performed using proton nuclear magnetic resonance (^{1}H-NMR) spectroscopy through comparing a+b integrals corresponding to the olefinic hydrogens of methacrylate (δ5.73 and δ6.15 ppm) with aromatic hydrogens present in the phenylalanine, tyrosine, and histidine (indicated by δ7.3–7.5 ppm) (Fig. 1b and c). The appearance of the olefinic hydrogens (a+d at δ = 5.8–6.2 ppm) and methyl hydrogens [3H's] (c at δ = 1.9 ppm) demonstrates the grafting glycidyl methacrylate to the gelatin backbone. The absence of aliphatic protons' peaks of epoxide ring (2H, -*O*-CH_2) at δ = 2.82 and 2.67 ppm indicates that the unreacted glycidyl methacrylate was completely removed from the product during dialysis and lyophilizing process (Fig. 1b and Supplementary Fig. S2) [47]. The Fourier-transform infrared (FT-IR) spectroscopy further demonstrated the formation of GELGYM with different FD (Supplementary Fig. S3). The appearance of the carbonyl absorption peak of methacrylate ester moieties manifested by a gradual increase in the intensity absorbance's ratio between the absorption peak at 1650 cm^{-1} and the un-modified characteristic absorption peak of secondary amides from gelatin at 1545 cm^{-1}, along with a spectral blue shift at 1650 cm^{-1} in FT-IR spectra further validated the formation of GELGYM with different FD (Fig. S3).

Table 1
Gelatin-based hydrogels prepared.

GELGYM] = 22.5% and CT = 5 min	**FD (%)**							
	2.6	11	24	57	107	157	169	175
[GELGYM] = 22.5% and FD = 175%	**CT (min)**							
	1	2	3	5	10	–	–	–
FD = 175% and CT = 5min	**[GELGYM] (%)**							
	7.5	10	15	20	22.5	–	–	

Owing to a high abundance of methacrylate functional moieties, GELGYM prepolymer has been shown to photocrosslink with visible light (505–515 nm) with very low intensity (20 mW/cm^2) in the presence of eosin Y (E), triethanolamine (TEA) and vinyl caprolactam (VC) through a radical reaction as previously has been explored to crosslink hydrogels such as GelMA [48] and poly(ethylene glycol) diacrylate (PEGDA) [49] (Fig. 1a). Visible light photopolymerization allows the dissociation of initiator molecules into free radicals that can react with the functionalized prepolymer. The kinetic of methacrylate polymerization through the generation of amino radicals by TEA is quite slow, so VC was added as a comonomer in the eosin-mediated photopolymerization to enhance the rate of radical polymerization and the final conversion of the polymer (Fig. S1a). The conversion of the polymer (reaction progress) can be monitored with the gradual decline in the integral of a+b hydrogen peaks, compared to aromatic hydrogens d) as a function of CT in ^{1}H-NMR spectra (Fig. 1b). Our analysis demonstrated a sigmoidal correlation between the crosslinking progress and irradiation time, where the reaction reaches to near completion in 10 min (Fig. 1d and Supplementary Fig. S4).

3.2. Mechanical properties

The mechanical properties of GELGYM were assessed by performing standard uniaxial tensile [50] and compression [43] experiments (Fig. 2a-p). Tensile measurements demonstrated that the tensile moduli, ultimate tensile, elongation, and energy at break (toughness) of GELGYM are strongly dependent on its FD. Varying FD, the tensile moduli of the hydrogel (5 min crosslinking, 22.5% w/w) could be tuned from 0.15 MPa (2.6% FD) to ≈ 1.25 MPa (175% FD), improving the mechanical behavior of other gelatin derivatives (0.18 MPa in the same settings for GelMA –Fig. 2a and b- and reported 0.22 MPa [30]). GELGYM hydrogels also showed the ability to withstand extremely high stresses before breakage, demonstrated by their high ultimate tensile up to 1.95 MPa (175% FD, 5 min crosslink, and 22.5% w/w), approaching those of the human cornea (6.9 MPa) compared to 0.1 MPa for GelMA in the same settings (Fig. 2a and d) and reported 0.05 MPa [28]. Moreover, the GELGYM hydrogels could be stretched up to 4.1-fold (Fig. 2a) of their initial length with the energy at break of up to 1.6 MPa (Fig. 2d), representing superior elasticity and toughness [51] compared to existing hydrogels such as GelMA (less than one-fold) (Supplementary Movie S1).

Moreover, our study indicated that varying CT (Fig. 2e–h) and GELGYM concentration (Fig. 2i-l) allows generating a library of GELGYM hydrogels with a wide range of mechanical properties (with the tensile moduli ranging from 0.034 to 1.45 MPa, ultimate tensile of 0.074–2.05 MPa, the toughness of 0.076–1.71 MPa and elasticity of 210–410%) that can be optimized according to biomedical needs. Compressive stress-strain measurements showed a similar trend, with the compressive moduli strongly dependent on the FD of gelatin, CT, and GELGYM concentrations (Fig. 2m–p). We showed that the compressive modulus of the hydrogel is programmable from 0.07 MPa (2.6% FD) to ≈ 0.46 MPa (175% FD) compared to 1.69 MPa for the human cornea and 0.19 MPa for GelMA in the same settings (Fig. 2m and n) and reported 0.15 MPa [52]. Compression tests also indicated that GELGYM hydrogels can dissipate energy effectively as shown by the pronounced hysteresis (Fig. 2m). While GELGYM with a lower FD showed a greater degree of hysteresis and dissipated more energy, those with higher FD were demonstrated to store more energy and had an elastic behavior. Moreover, GELGYM hydrogels were able to withstand compressive strains as high as 80% without breaking, recovering to the initial state

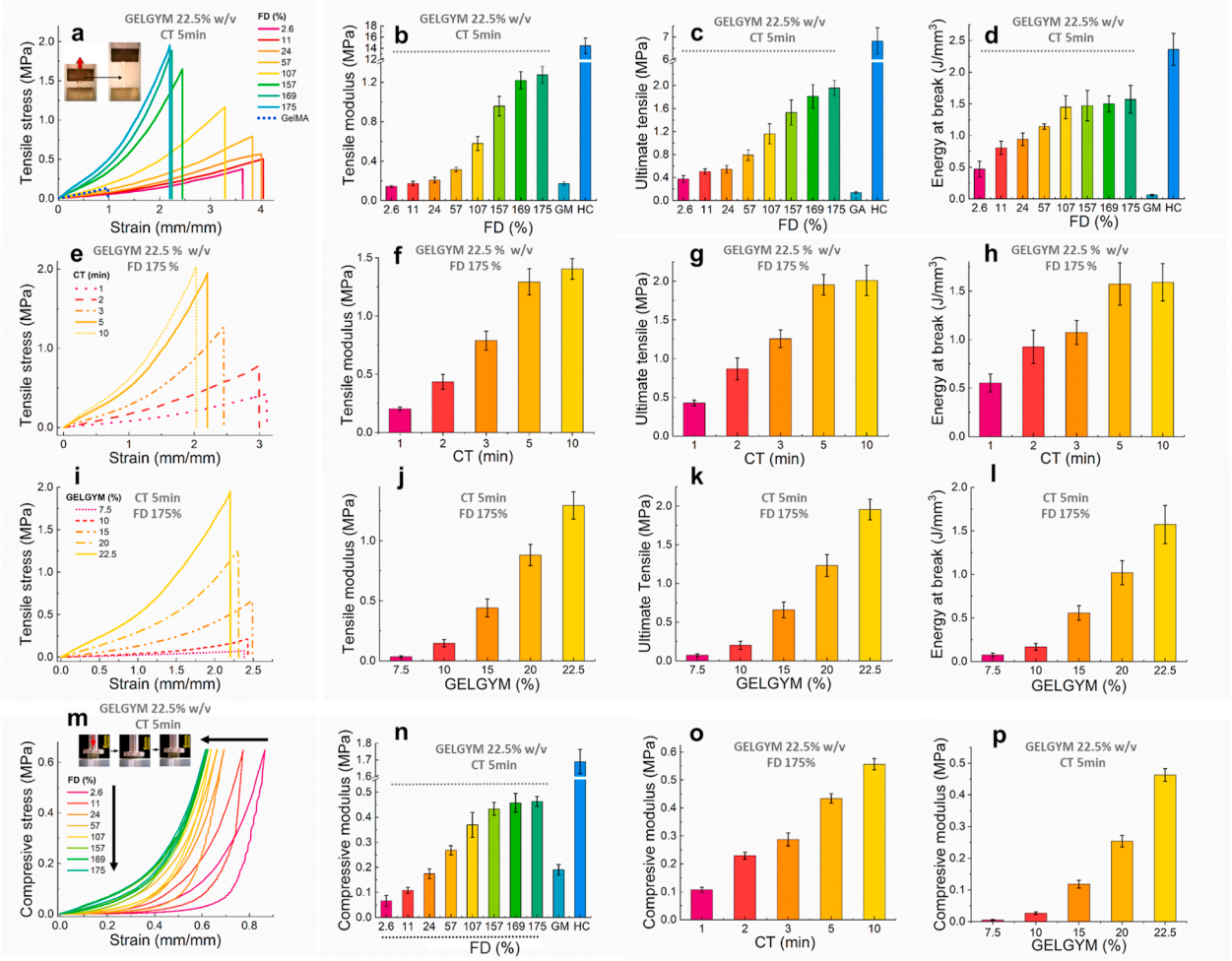

Fig. 2. Mechanical characterization of GELGYM. a) Representative tensile stress/strain curves for GELGYM (22.5% w/v and crosslinked for 5 min) with varying FD and their corresponding mean tensile modulus (b), ultimate tensile (c) and energy at breaks (d), compared to those of GelMA (GM) and fresh human cornea (HC). (The inset in (a) demonstrates the unique elasticity of GELGYM). e) Representative tensile stress/strain curve of GELGYM hydrogels (FD of 175% and 22.5% w/v) with varying CT and their corresponding mean tensile modulus (f), ultimate tensile (g), and energy at breaks (h), compared to those of GelMA and fresh human cornea. i) Representative tensile stress/strain curve of GELGYM hydrogel (FD of 175% and crosslinked for 5 min) with varying concentration and their corresponding tensile modulus (j), ultimate tensile (k), and energy at breaks (l), compared to GelMA and fresh human cornea. (m) Representative compressive stress/strain curves for GELGYM (22.5% w/v and crosslinked for 5 min) with varying FD. The mean compressive modulus of GELGYM with varying FD (n), CT (o), and concentration (p), compared to those of GelMA and fresh human cornea. (The inset of (m) demonstrates the unique compressibility of the GELGYM).

without deformation (Fig. 2m). Furthermore, the compressive moduli of GELGYM could be programmed from 0.004 to 0.56 MPa via varying CT (Fig. 2o) and prepolymer concentration (Fig. 2p). Such 5–10 folds enhancement of mechanical properties (tensile modulus, tensile strength elongation at breaks, toughness, and compression modules) is believed to originate from an enhanced FD and subsequent greater crosslinking density. Moreover, the superior elasticity is attributed to the formation of the longer linker between the gelatin backbones and the capacity to create hydrogen bonds formed between hydroxyl groups of the gelatin network and solvent [43].

3.3. Structural and optical properties

Hydrogel degradation and dissolution over time often result in attenuation of the hydrogel, unless there is counteracting tissue remodeling and regeneration [1]. Therefore, the stability of hydrogel is a key component to define its biomedical applications. To evaluate the stability of the hydrogel against enzymatic degradation, we incubated the GELGYM in a solution containing collagenase and compared the dried mass of the sample to the initial dried mass as a function of time [33]. Our data indicated that the biodegradation of the hydrogel can be easily controlled from 6 to 26 h through varying CT (longer CT leads to higher stability), approaching that of the native porcine cornea (Fig. 3a).

This higher stability is also attributed to the improved crosslinking density of GELGYM, which might restrict the accessibility of the enzyme to the cleavage sites of the hydrogel, along with increasing the anchoring points of cleavable units in the gelatin backbone. We also studied the swelling behavior of the hydrogel in PBS solution for up to 4 days at 37 °C in an incubator. The swelling ratio was shown to vary from 13 to 90% of the original size, depending on the CT of GELGYM (longer CT leads to lower swelling ratio) (Fig. 3b). This is consistent with the prior mechanical evaluations and can be attributed to the varying crosslinking density between gelatin chains. The swelling degree allowed for the determination of the crosslinking density and the average molecular weight between nodes [53], parameters which define the three-dimensional network structure of hydrogels. Considering the Flory-Tehner equation, the average molecular weight between nodes (M_c) can be determined (Eq. (1)) assuming that in the equilibrium state

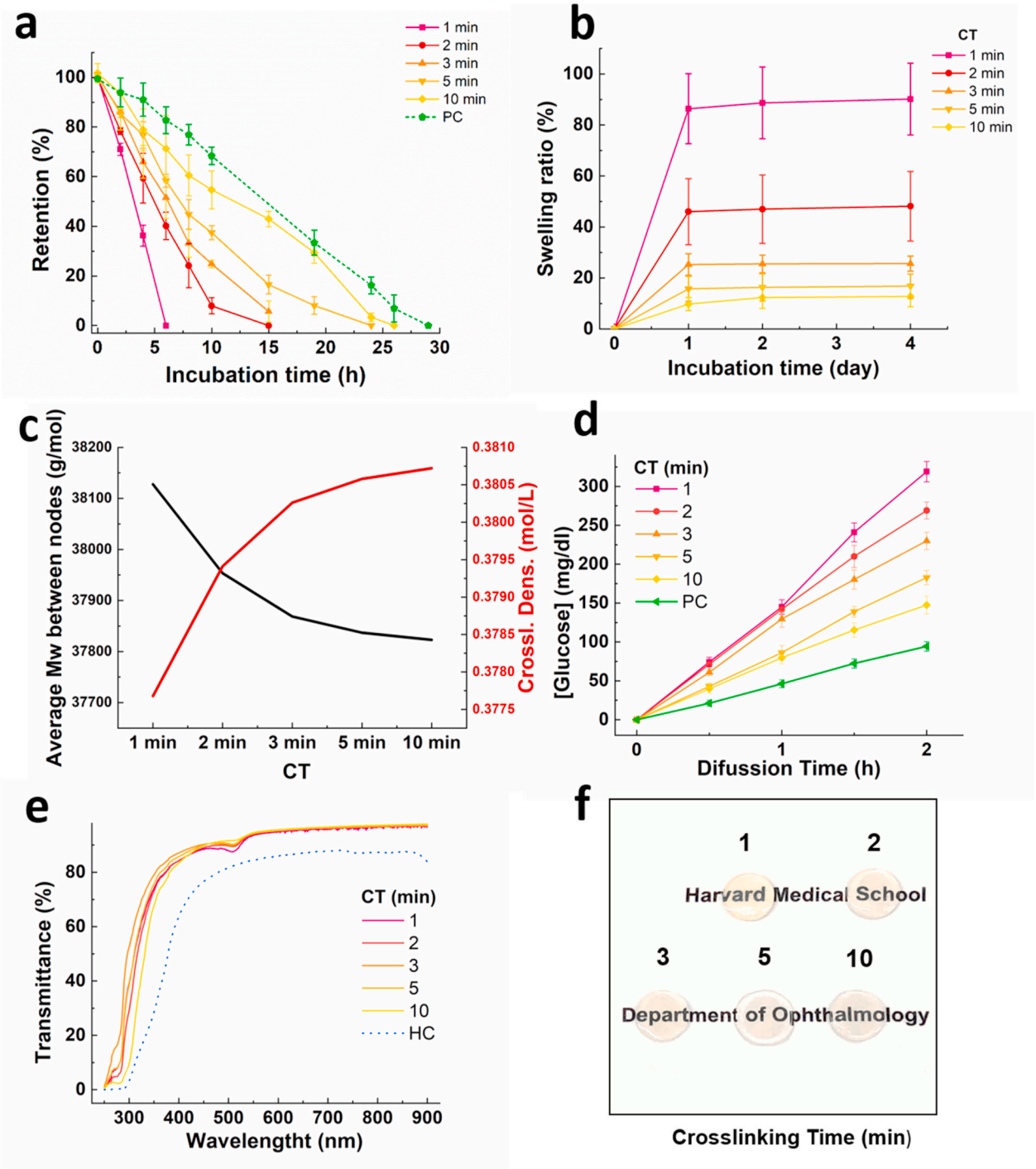

Fig. 3. Structural and optical properties of GELGYM. a) Collagenase induced degradation rate of GELGYM hydrogels (FD of 175% and 22.5% w/v) with varying CT from 1 to 10 min as a function of incubation time (T = 37 °C and 5% CO_2). b) Swelling ratio of GELGYM hydrogels (FD of 175% and 22.5% w/v) with varying CT from 1 to 10 min. c) Crosslinking density and an average molecular weight between nodes of gelatin-based hydrogels at different crosslinking times. d) Glucose permeability and e) optical transmittance of GELGYM hydrogels (FD of 175% and 22.5% w/v) with varying CT from 1 to 10 min in the range on 250–850 nm. f) GELGYM transparency images at different crosslinking times. PC: porcine cornea; HC: human cornea.

the sum of free energies is zero:

$$\frac{1}{Mc} = \frac{2}{Mn} - \frac{\frac{v\left[\ln(1-v2,s)+v2,s+\chi v^2 2,s\right]}{V1}}{V2,s^{1/3} - \sqrt{\frac{v2,s}{2}}} \quad (1)$$

Where M_n is the number average molecular weight of gelatin, v is the specific volume of the dry polymer, V_1 corresponds to the molar volume of the solvent (18.1 mL/mol for water), v_2,s is the polymer volume fraction at equilibrium, and χ is the Flory–Huggins solvent-polymer interaction parameter (0.49 ± 0.05 for Gelatin-water interaction) [54]. From the values of the average molecular weight between nodes (M_c), the crosslinking density (ρ_x) can be calculated (Eq. (2)), which is defined as the average number of polymer units between two consecutive nodes. A low crosslinking density gives rise to a more open network and a higher degree of hydration. However, a high crosslinking density implies a lower degree of hydration and a less deformable hydrogel.

$$\rho_x = \frac{1}{v^* M_c} \quad (2)$$

The M_c and the crosslinking density (ρ_x) values are shown in Fig. 3c. Increasing the crosslinking time M_c decreases, that is, the molecular weight between two consecutive nodes decreases, while the crosslinking density increases.

Permeability studies revealed that the GELGYM has a higher glucose diffusion rate compared to native tissue, which also has shown to depend on the CT of the hydrogel and crosslinking density (Fig. 3d and Supplementary Fig. S5 and section 2). Although the GELGYM crosslinked for 10 min swelled nearly 25% after 4 days incubation in PBS at 37 °C, it showed higher glucose diffusion compared to the native tissue, as shown in Fig. 3d.

Such aforementioned structural properties should facilitate the application of GELGYM in a wide range of biomedical areas including ophthalmology, where globally there is a severe scarcity of donor corneas, due to issues of tissue suitability and microbial contamination. Despite significant progress to engineer artificial scaffolds, past efforts have to date fallen short in emulating mechanical, chemical, and other biomimetic characteristics of the native cornea [55,56]. To test the suitability of GELGYM in ophthalmological applications, we next evaluated the optical transmission of GELGYM using ultraviolet–visible (UV–Vis) spectroscopy in the range of 250–850 nm. Our data suggest that GELGYM has similar transparency to the human cornea (Fig. 3e). We observed that the hydrogels crosslinked for shorter period of time are pale yellow, as opposed to those crosslinked for longer period of time that are almost colorless. Moreover, increasing the CT imparted a positive effect in blocking UV light (200–350 nm) as shown in Fig. 3e and f.

3.4. In vitro biocompatibility

We further performed in vitro cell biocompatibility studies (2D-cell culture) to demonstrate that GELGYM crosslinked hydrogels can mimic the native cell-ECM interactions using different corneal cell cultures. For that purpose, we evaluated the interaction of HCEp, HCF, HCEn, and NDC with the engineered GELGYM as a function of CT. This enabled us to consider the effect of structural properties of GELGYM with different crosslinking densities on the cellular biocompatibility of the hydrogel. Standard Live-Dead assays indicated that all four types of cells were able to maintain nearly 100% viability after 48-h cell culture on GELGYM, independently of CT (i.e. 3, 5, and 10 min) (Fig. 4a and Supplementary Fig. S6). Similar to tissue culture plate (TCP), in vitro cultured cells were able to spread, migrate, and proliferate on GELGYM, reaching full confluency in less than 6 days. The metabolic activities of all four types

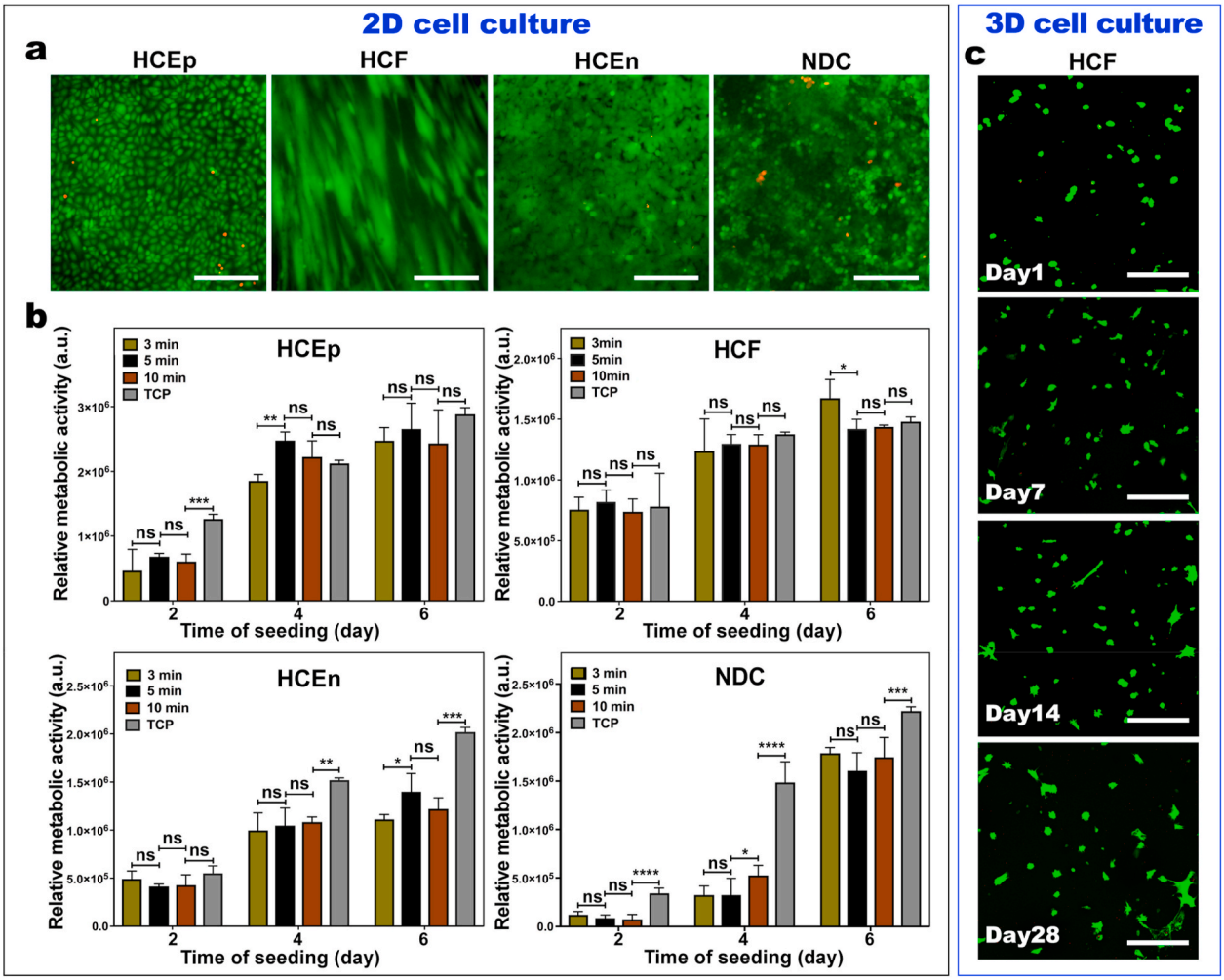

Fig. 4. In-vitro biocompatibility of GELGYM. a) Representative live-dead images of the human corneal epithelial cells (HCEp), corneal fibroblasts (HCF), and corneal endothelial cells (HCEn) along with hybrid neuroblastoma cells (NDC) cultured on GELGYM hydrogels (FD of 175% and 22.5% w/v and 5 min crosslinking) after 6-day incubation. b) Quantification of metabolic activity using AlamarBlue assay for HCEp, HCF, HCEn, and NDC cultured onto GELGYM hydrogels with varying CT from 3 to 10 min, compared to the cells seeded on the TCP after 2, 4 and 6 days of incubation (ns, *, **, ***, and **** represent $p > 0.05$, $p < 0.05$, $p < 0.01$, $p < 0.001$ and $p < 0.0001$). c) Representative stacked confocal live-dead images of HCF, 3-dimensional (3D) cultured within GELGYM hydrogels (FD of 175%, 10% w/v and 5 min CT), during 1 month of incubation. (Green [calcein AM]: lived cells; Red [ethidium homodimer-1]: dead cells). Scale bar: 200 μm.

of cells cultured on GELGYM with varying CT were also quantified using AlamarBlue assay (Fig. 4b). All of the studied cells exhibited a significant increase in relative fluorescence intensity as a function of incubation time, yet with a distinctive pattern, suggesting enhanced cellular activity and proliferation rate over time.

Although the metabolic activities of the HCEp and HCF cells cultured on GELGYM were statistically similar to those on TCP (control) in all time points, HCEn and NDC cells showed lower metabolic activities on GELGYM compared to those on TCP. Lower metabolic activities are directly proportionate to the cell number at any particular time point and rate of proliferation. HCEn culture is sensitive for the attachment on the culture surfaces. Usually FNC coating of the surface was done before HCEn culture as it was previously shown that FNC coating mix significantly reduces cell loss during rinsing [57]. However, in our study we did not use FNC coating as it was previously showed that HCEn prefer to growth of TCP with or without coating compare to hydrogel with or without FNC [58]. Our result of low HCEn growth on hydrogels is similar to previous published reports.

NDC rate of proliferation is highly regulated by the surface chemistry of the culture surface. The authors of this manuscript previously showed that, even on collagen surface, which is considered the standard surface for cells culture, NDC proliferation can be altered by adding cell specific peptide motif inside the collagen hydrogel [59]. In our case, we found less proliferation for NDC compare to TCP which might be possible to overcome by adding specific peptides into the hydrogel. However, cell numbers on GELGYM hydrogels were similar.

While it has been shown that the mechanical properties of the substrate influence the cell adhesion, proliferation, and differentiation [60], we did not witness any salient differences between the proliferation rates of cells cultured on GELGYM crosslinked for different periods, suggesting the insensitivity of biocompatibility to varying structural properties in the studied ranges (Supplementary Fig. S6). The biologically active matrix of GELGYM, along with its ease and biosafety of processing, led us to evaluate the potential of the hydrogel in 3D-cell culture. Our data showed that encapsulated fibroblasts not only retain high viability, but also spread with different rates corresponding to the varying CT, as demonstrated by standard Live-Dead assay (Fig. 4c and Supplementary Figs. S7 and S8).

In recent years, cells encapsulation into biocompatible hydrogels has drawn keen scientific interest, but still remains very challenging. Although crosslinking prevents hydrogel shrinkage, immediately after cell encapsulation the small mesh size of these highly crosslinked hydrogels prevents cell spreading, and results in cells with round morphology which ultimately delays cell proliferation, migration, and matrix production [61–63]. Several approaches have been investigated for increasing cellular biocompatibility of encapsulation biomaterials [64,65]. Gelatin based hydrogels have been previously used for cell encapsulation. Higher cell viability was observed previously with collagen compared with GelMA cell encapsulation [66]. Similar to our observation when fibroblasts encapsulated in gelatin hydrogel were prepared by UV irradiation, most of the encapsulated cells survived and almost no dead cells were found, meaning that gelatin based biomaterials are not cytotoxic and suitable for further cell encapsulation [67]. High cell survival is related to the biocompatible nature of gelatin which provides active attachment point to the cells and the microporous structure of hydrogels to facilitate the efficient transportation of nutrients, water, and oxygen throughout the matrix [67]. We hypothesized that cell survival is very important in the cell encapsulation as we observed even on day 28, that most of our cells survived. In a real (*in vivo*) scenario, due to photolytic activity, biomaterials will loosen and cells will have more room to spread. However, in vitro data showed that fibroblast spreading can be improved inside a hydrogel by making interpenetrating networks (IPNs) with hyaluronic acid (HA) [68]. Increasing cell spreading early in our hydrogels through IPNs can be studied in the future.

The 2D and 3D cell culture further validates the biomimetic properties of GELGYM to emulate native ECM and provide a biologically active microenvironment to support cell-matrix and cell-cell interactions.

3.5. Ex vivo biocompatibility and retention

To evaluate the ex vivo retention of the hydrogel after application in the corneal tissue, we applied GELGYM as a filler-adhesive to attach two human corneoscleral limbal pieces and incubated them under specific culture conditions (Fig. 5a). Our study showed that the retention rate of attachment under culture (at 37 °C) was 100% for 6 months of study (Fig. 5b). We also noticed that full stratified epithelialization of the glued area took place in less than a week, yet fibroblast migration into GELGYM happened more slowly. TEM demonstrated the presence of fibroblasts into GELGYM after a 1-month incubation. Moreover, simultaneous degradation of the hydrogel and the formation of new collagen fibers secreted from migrated fibroblasts into GELGYM were also observed by TEM, indicating synchronized degradation and biointegration processes. Such continuous processes led to the replacement of the GELGYM scaffold with newly synthesized collagen, leading to attachment and unification of the two pieces, as indicated by TEM after 6-month culture (Fig. 5c). Phenotypic evaluation of the HCEp and HCF in GELGYM was performed by immunohistochemistry. Our data revealed that HCEp on the glued area expressed cytokeratin 3 + 12 (specific corneal epithelial markers) (Fig. 5d) [69,70]. It was also shown that migrated HCF expressed ALDH3A1 protein (corneal fibroblast marker), without expressing α-SMA (myofibroblast marker, the latter associated with a fibrotic response) [71]. In addition, HCEn cultured on the GELGYM scaffold expressed ZO-1 (corneal endothelial marker associated with the presence of tight junctions) (Fig. 5e) [72], further validating the biomimetic characteristics of the engineered hydrogel.

Depending on the type of treatment, biomaterials come in contact with blood either continuously or during implantation. This is not only the common scenario for vascularized organs such as the liver or kidney, but also for the cornea in severe diseases that cause corneal neovascularization. Thereafter, the implanted materials will be exposed to recognition molecules of various branches of innate immunity. Among these systems are the plasma cascades, of which the complement system is one of the fundamental parts, playing a crucial role in homeostasis, regeneration, and inflammation [38]. To evaluate the potential of complement to be activated by GELGYM in human blood, we measured two activation fragments of the complement system (Fig. 5f). One, C3bc, at C3-level where C3 is cleaved into C3a and C3b, which is further cleaved to C3c and C3dg; and another at the terminal level where the C5b-fragment binds to C6, C7, C8, and several C9 molecules to form the terminal complement complex C5b-9 (TCC), which when formed in the fluid phase is a highly reliable indicator of complement activation, and thus reflects biocompatibility [73].

We found that the level of C3bc and soluble TCC were significantly higher in the presence of GELGYM compared to background activation (Fig. 5f). This result demonstrates that GELGYM is a complement activating material. Extensive research into complement protein C3a has revealed its roles in bone marrow engraftment and hematopoietic stem cell mobilization. Progenitor cells including myeloid, erythroid, and megakaryocytic blasts, as well as human $CD34^{+}$ cells, were all found to express the C3a receptor (C3aR) [38]. On one hand, increasing evidence suggests that complement activation may be beneficial in bone replacement surgery to enhance tissue regeneration and integration of the orthopedic biomaterials [38]. On the other hand, uncontrolled activation may trigger inflammatory and thrombotic reactions leading to implant failure. Thus, it is still unclear to what extent complement activation is beneficial or harmful for the integration of an implanted material [74]. For some implantations, the absence of complement activation and subsequent cytokine release are necessary for the implanted “organ” to survive. In other situations, e.g., an artificial orthopedic device made of metal, a modest complement activation with a

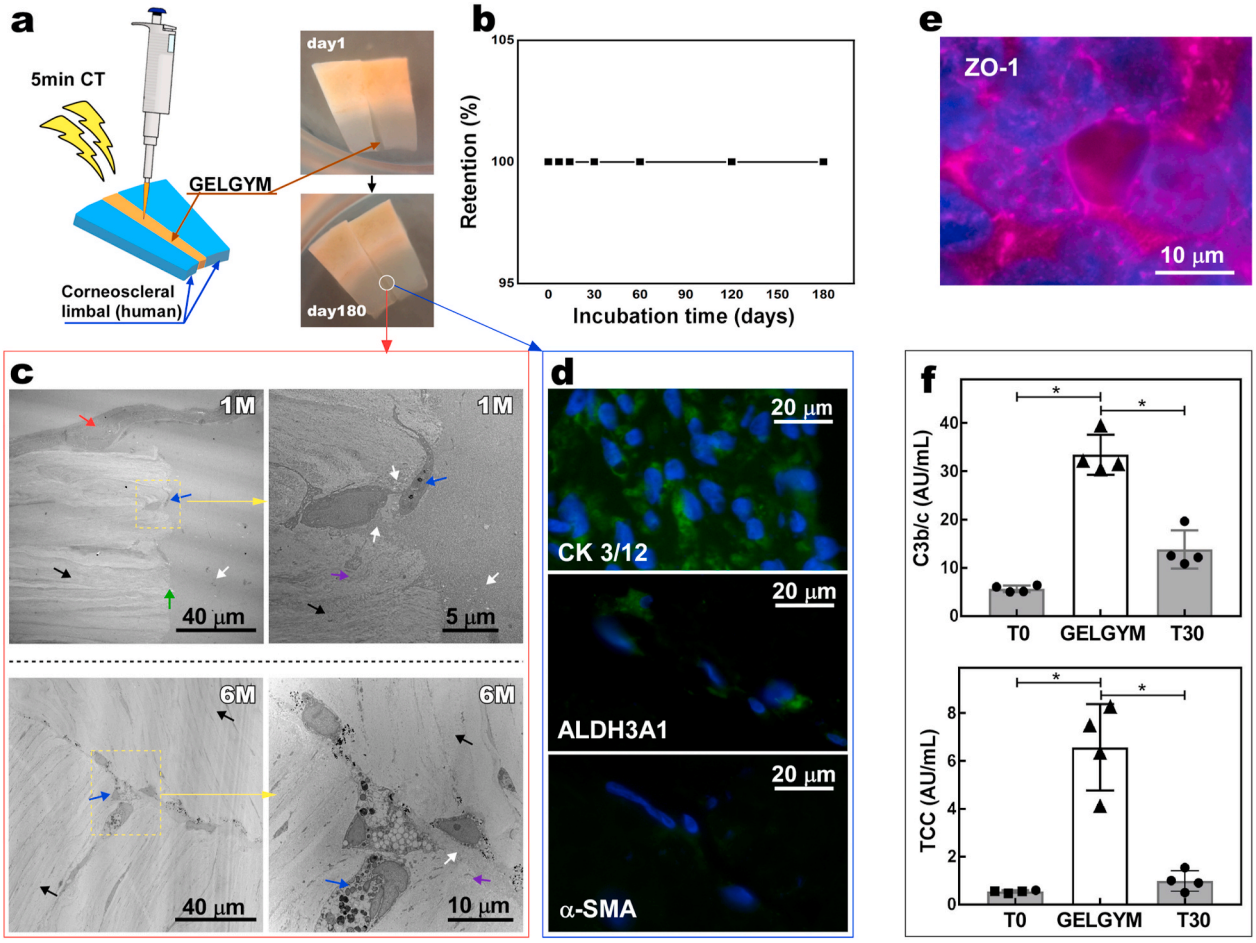

Fig. 5. Ex vivo retention and biocompatibility of GELGYM. a) Application of GELGYM as glue to attach two human corneoscleral limbal pieces (FD of 175% and 22.5% w/v and 5 min crosslinking) and their retention rate (b) as a function of incubation time (T = 37 °C and 5% CO_2). c) Representative TEM images of the cross-sectional interface of tissue-glue after 1 and 6-month incubation in culture media (the red and blue arrows show the stratified HCEp and HCF respectively (the white and black arrows illustrate GELGYM and highly organized collagenous fibers of the tissue, respectively, separated by the interface [green arrow]. The violet arrow shows newly synthesized and partially organized collagen fibers as the GELGYM is biodegraded by HCF, indicating tissue regeneration). d) Fluorescent immunostaining images of the cross-sectional interface after 6-month incubation in culture media, showing the expression (green signal) of CK 3/12 in HCEp (top), ALDH3A1 in HCF (middle), and α-SMA in HCF (bottom); all cell nuclei were counterstained using DAPI (blue). e) Representative fluorescent immunostaining image of HCEn cultured on GELGYM, after 6 days, indicating the expression of ZO-1 (pink signal). f) Complement activation by GELGYM, noted by an increased level of C3bc and soluble terminal complement complex (sC5b-9) compared to the background activation after 30 min (T30). (T0 represents the status of complement activation immediately after drawing the blood from the donor (*$p < 0.05$)).

subsequent controlled inflammatory response could indeed benefit attachment to surrounding tissue. Thus, if the inflammatory reaction remains below the level at which tissue damage occurs, it might benefit integration and adhesion, reducing late loosening of the device.

3.6. Adhesion properties

We further investigated the application of GELGYM as a glue for corneal wound closure, currently achieved by the application of sutures. Suture material can be associated with irritation, inflammation, infection, and may lead to neovascularization and astigmatism [75]. Despite substantial efforts to design an effective adhesive to close corneal incisions, none of the currently existing materials applied in clinical settings are capable of meeting those requirements [76]. For instance, fibrin glue lacks required mechanical properties, degrades quickly, and may lead to immunological reactions [77]. PEG-based adhesives seal corneal incisions, yet are incapable of filling stromal defects, lack cell adhesion, and fall off quickly [78]. Cyanoacrylates, while effective for treating small corneal perforations (<3 mm in diameter), have low biocompatibility and are non-degradable [77], causing neovascularization and inflammation [79]. ReSure® is an FDA-approved PEG-based ocular adhesive and used to seal corneal incisions in cataract surgery. However, it is unable to fill stromal defects and falls off quickly (less than 3 days) [38]. GelMA has also been proposed in preclinical studies as a corneal bioadhesive and stromal substitute, demonstrating its suitability for short-term wound closure [30,80]. To evaluate the potential of GELGYM in ophthalmic surgery as an adhesive, we examined the adhesion strength of the hydrogel to corneal tissue using the adopted burst pressure test (Fig. 6 and Supplementary Fig. S9).

Our ex vivo data revealed that GELGYM can seal full penetrating corneal defects of up to 4 mm-diameter (Fig. 6b) when used as a pre-polymer solution. However, GelMA and cyanoacrylate could only seal 2-mm perforations in similar settings as also reported by others [38]. Moreover, we demonstrate that GELGYM can function as a tissue adhesive and attach either a corneal graft or pre-crosslinked GELGYM patch to larger perforations (e.g. 6–8 mm), tolerating pressures as high as 200 mmHg. Moreover, our studies revealed that increasing CT significantly improves the adhesion strength of GELGYM. Considering these properties, we envision GELGYM to have the potential to satisfy various needs in ophthalmology including, (i) as an adhesive sealant for corneal or corneoscleral lacerations facilitating an instant primary closure, (ii) as a corneal glue for facilitating sutureless grafting in

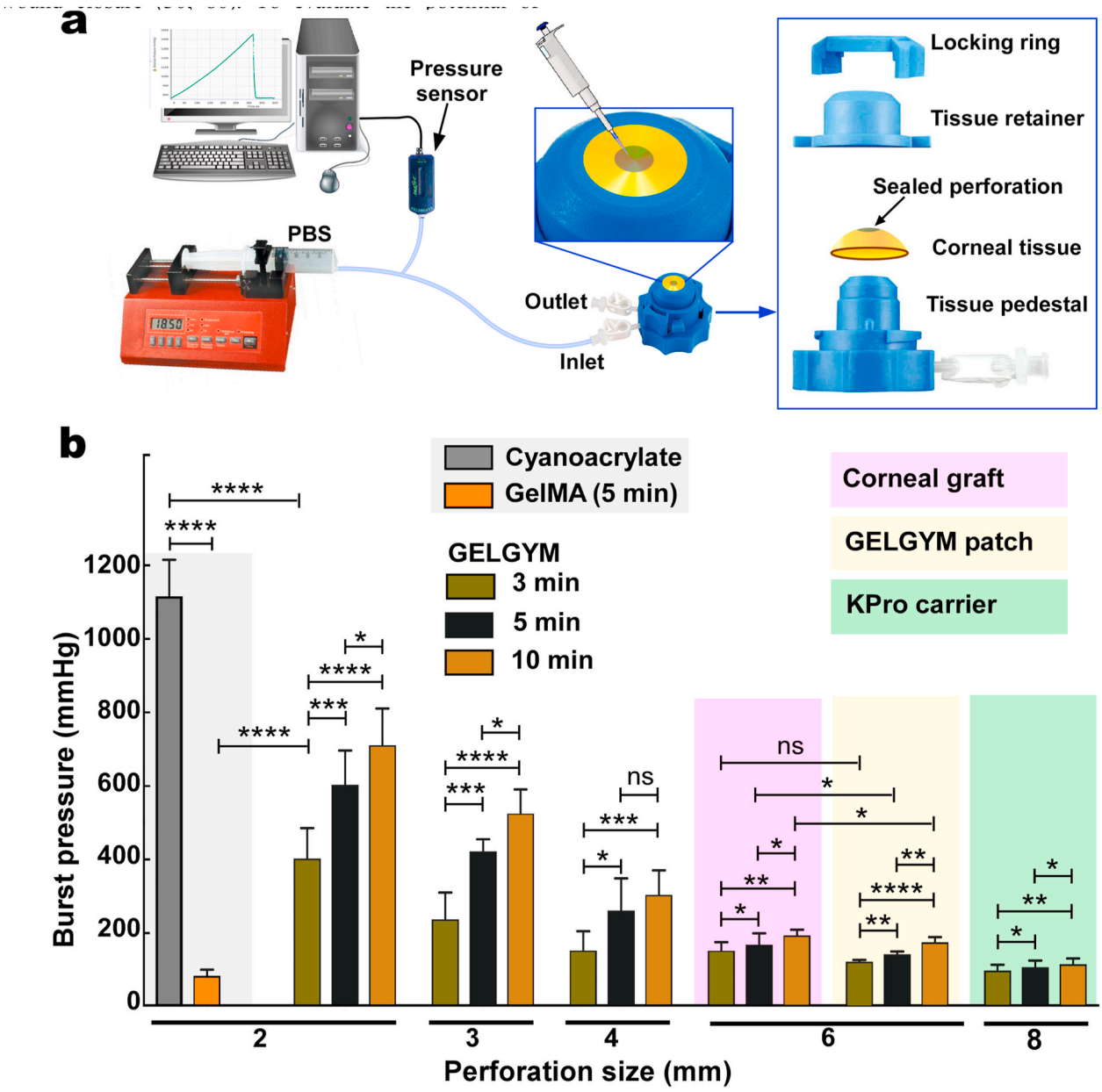

Fig. 6. Ex-vivo burst pressure test of GELGYM. a) Burst pressure set-up for measuring the adhesion properties of GELGYM to seal corneal perforations ranging from 2 to 8 mm. The perforated corneas were placed between the pedestal and the tissue retainer, and secured by locking ring (FD of 175% and 22.5% w/v) for varying perforations, application approaches and CT, compared to GelMA and cyanoacrylate glue (ns, *, **, ***, and **** represent $p > 0.05$, $p < 0.05$, $p < 0.01$, $p < 0.001$ and $p < 0.0001$).

anterior, endothelial and penetrating keratoplasties, and (iii) as a corneal stromal substitute or filler to generate an immediate sutureless keratoplasty without the need of a donor corneal stroma in anterior lamellar and penetrating keratoplasties, including keratoprosthesis implantation (Fig. 7a, and Supplementary Fig. S10 and Movies S2–S3) and other biomedical applications (Fig. 7a and Supplementary Fig. S10).

As a proof of concept, we performed a lap shear test to study the adhesion of GELGYM with various dynamic biological surfaces (Fig. 7b and c) and have shown that GELGYM can strongly adhere to the wet surface of the aorta, heart, muscle, kidney, liver, and spleen, comparing to the tensile strength of commonly used surgical sutures (Fig. 7c) and superseding by far, the adhesion strength of most of the widely used adhesives such as fibrin glue (Evicel®) and PEG-based adhesive (Duraseal®) with a shear strength of 0.1 and 0.6 N/cm^2, respectively (Fig. 7b and c and Supplementary Movie S4) [81]. Such adhesion is believed to arise from the diffusion of GELGYM into the collagenous tissue followed by radical polymerization, which leads to strong mechanical anchoring inside the tissue along with non-specific radical initiated crosslinking through the lysine amino acids of the host collagen and hydrogen-bonding, electrostatic and hydrophobic interactions. Such mechanical anchoring also explains why the higher CT leads to enhanced adhesion properties indicated by the burst pressure test (Fig. 6).

To expand the applications of GELGYM, we also engineered an artificial blood vessel and showed that it can tolerate pressures as high as 350 mmHg before failure (Supplementary Fig. S10 and Movie S5). These studies validate the excellent mechanical, structural, biological, and adhesive properties of GELGYM, and suggest versatile functions for this modified biomaterial in several biomedical applications

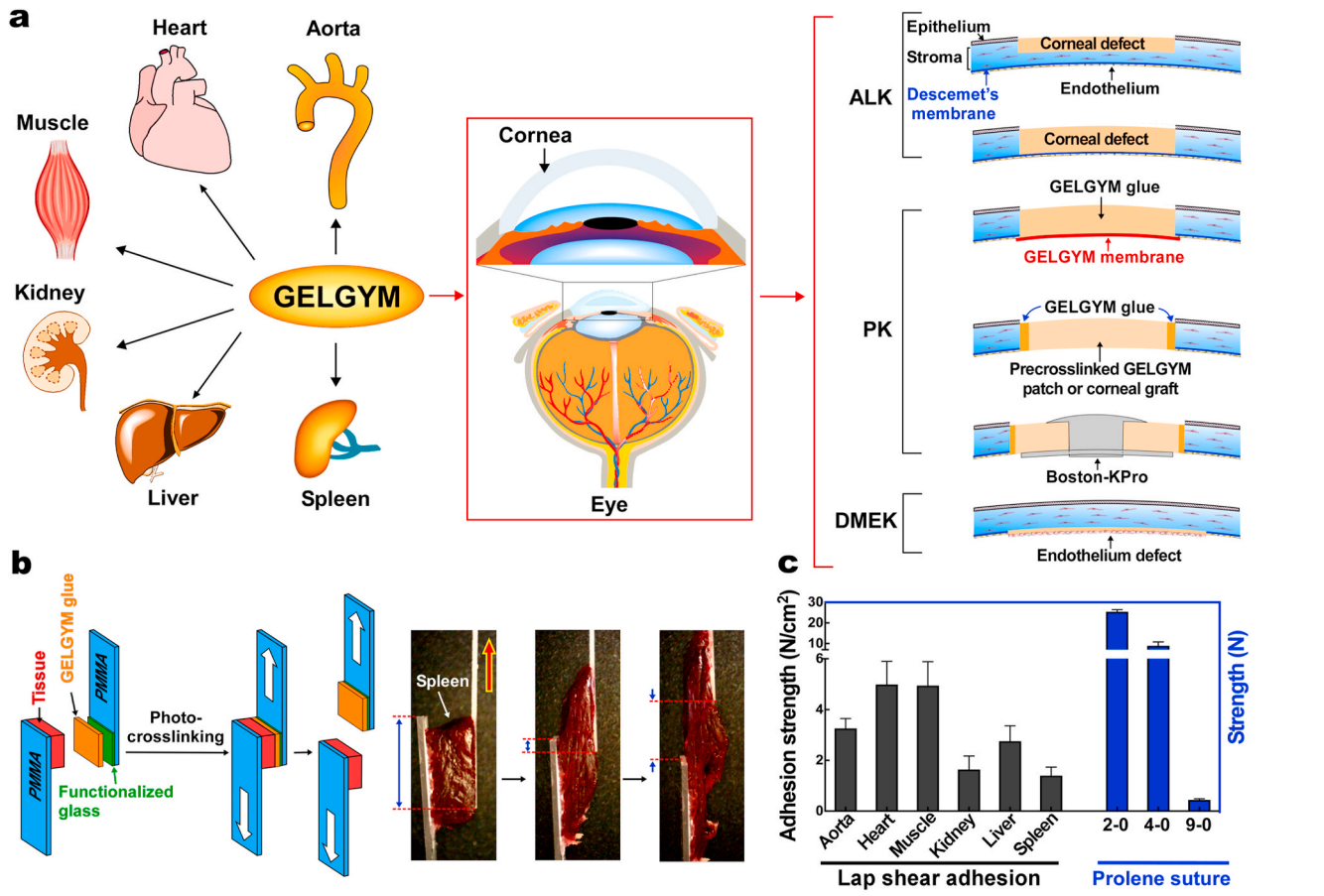

Fig. 7. Biomedical applications of GELGYM. a) Various potential applications of GELGYM in biomedical engineering including ophthalmology such as Anterior Lamellar Keratoplasty (ALK), Penetrating Keratoplasty (PK), including Boston-Keratoprosthesis implantation (Boston-KPro), and Descemet Membrane Endothelial Keratoplasty (DMEK). b) Lap shear set-up and (c) the corresponding adhesion strength of GELGYM with different organs compared to the strength of traditional surgical Prolene® sutures.

4. Conclusion

In this report, we engineered a versatile hydrogel with strong adhesion to biological surfaces. It is biocompatible with a wide range of structural characteristics, controlled by varying FD, CT, and prepolymer concentration, allowing customizable properties according to the specific medical needs. These, along with ease and biosafety of processing (crosslinked with low intensity of visible light and low concentration of the crosslinking reagents) to create cellularized constructs (i.e. 3D cell encapsulated and/or cells cultured on GELGYM surface) further emphasize the potential applications of GELGYM not only in ophthalmology but also in other medical areas. Thus, GELGYM might act as bioadhesive (e.g. tissue sealant, immobilizing medical devices, etc.), and also as a tissue-engineered scaffold or biomaterial for 3D-bioprinting, wound dressing, cell and gene delivery, differentiation studies, drug development, and controlled delivery, cancer research or cell physiology, among others [82].

Supporting information

Supplementary data related to this article is available free of charge via the Internet at https://iopscience.iop.org.

Author contributions

R.S. conceived and executed the synthesis process. R.S. and H.S. performed the structural properties studies. R.S., R.I., M.G-A., and M.M. I. conducted the biocompatibility tests and retention studies. D.K. executed NMR and IR experiments. R.S. prepared the manuscript. F.R-O conducted the crosslinking parameters calculations, re-analyzed the FTIR data. D.A-M improved figures and presentation of the manuscript. P.H.N., T.E.M., C.H.D., J.C., F.R-O, D.A-M, and M.G-A. discussed results and revised the manuscript. M.G-A. supervised the project and corrected the manuscript for publication. All authors commented on the final draft.

Funding sources

This paper was supported by the Boston-KPro research fund and NIH/NEI P30EY003790 (Core-PA). R.S. was supported in part by the K99 grant from NIH award no. K99 EY030553. This work was performed in part at the Center for Nanoscale Systems (CNS), Harvard University, a member of the National Nanotechnology Coordinated Infrastructure Network (NNCI), which is supported by the National Science Foundation under NSF award no. 1541959. F.R-O and D.A-M were supported by the research project ICI19/00006, funded by Instituto de Salud Carlos III and co-funded by European Union (ERDF/ESF, "A way to make Europe"/"Investing in your future"). F.R-O additionally acknowledges funding from *Plan Andaluz de Investigación, Desarrollo e Innovación (PAIDI2020)* Fellowship supported by *Consejería de Economía, Conocimiento, Empresas y Universidad, Junta de Andalucía* co-funded by *Fondo Social Europeo de Andalucía 2014-2020*.

Acknowledgements

The authors wish to thank Ann Tisdale and Philip Seifert for helpful

discussions and TEM/SEM data acquisition, and VisionGift (Boston, MA) for kindly providing human corneal tissue.

Appendix A. Supplementary data

Supplementary data to this article can be found online at https://doi.org/10.1016/j.bioactmat.2021.03.042.

Abbreviations

^{1}H-NMR	proton nuclear magnetic resonance
BSA	bovine serum albumin
CT	crosslinking times
E	eosin Y
FBS	fetal bovine serum
FD	functionalization degree
GELGYM	gelatin glycidyl methacrylate
GelMA	gelatin methacryloyl
HCEn	corneal endothelial cells
HCEp	human corneal epithelial cells
HCF	corneal fibroblasts
ICC	immunocytochemistry
IHC	immunohistochemistry
MMC	macromolecular microsphere composites
NDC	hybrid neuroblastoma cells
PAA	poly(acrylic acid)
PEG	poly(ethylene glycol)
PEGDA	poly(ethylene glycol) diacrylate
PGSA	poly(glycerol-*co*-sebacate acrylate)
PMMA	poly(methyl methacrylate)
PR	Polyrotaxane
TBS	tris-buffered saline
TCC	terminal complement complex C5b-9
TCP	tissue culture well plate
TEA	triethanolamin
TEM	transmission electron microscopy
UV–Vis	ultraviolet–visible
VC	vinyl caprolactam
VSNPs	hybrid silica nano-particles

References

[1] K.Y. Lee, D.J. Mooney, Hydrogels for tissue engineering, Chem. Rev. 101 (7) (2001) 1869–1879.

[2] J. Leijten, J. Seo, K. Yu, G. Trujillo-de Santiago, A. Tamayol, G.U. Ruiz-Esparza, et al., Spatially and temporally controlled hydrogels for tissue engineering, Math. Sci. Eng. R 119 (2017) 1–35.

[3] K.M. Galler, L. Aulisa, K.R. Regan, R.N. D'Souza, J.D. Hartgerink, Self-assembling multidomain peptide hydrogels: designed susceptibility to enzymatic cleavage allows enhanced cell migration and spreading, J. Am. Chem. Soc. 132 (9) (2010) 3217–3223.

[4] M.C. Cushing, K.S. Anseth, Hydrogel cell cultures, Science 316 (5828) (2007) 1133–1134.

[5] S.J. Jeon, A.W. Hauser, R.C. Hayward, Shape-morphing materials from stimuli-responsive hydrogel hybrids, Acc. Chem. Res. 50 (2) (2017) 161–169.

[6] L.J. Woo, K.S. Yeon, K.S. Soo, L.Y. Moo, L.K. Hyun, K.S. Jeong, Synthesis and characteristics of interpenetrating polymer network hydrogel composed of chitosan and poly(acrylic acid), J. Appl. Polym. Sci. 73 (1) (1999) 113–120.

[7] B.B. Mandal, S. Kapoor, S.C. Kundu, Silk fibroin/polyacrylamide semi-interpenetrating network hydrogels for controlled drug release, Biomaterials 30 (14) (2009) 2826–2836.

[8] D. Myung, D. Waters, M. Wiseman, P.E. Duhamel, J. Noolandi, C.N. Ta, et al., Progress in the development of interpenetrating polymer network hydrogels, Polym. Adv. Technol. 19 (6) (2008) 647–657.

[9] T. Huang, H.G. Xu, K.X. Jiao, L.P. Zhu, H.R. Brown, H.L. Wang, A novel hydrogel with high mechanical strength: a macromolecular microsphere composite hydrogel, Adv. Mater. 19 (12) (2007) 1622–+.

[10] F.K. Shi, X.P. Wang, R.H. Guo, M. Zhong, X.M. Xie, Highly stretchable and super tough nanocomposite physical hydrogels facilitated by the coupling of intermolecular hydrogen bonds and analogous chemical crosslinking of nanoparticles, J. Mater. Chem. B 3 (7) (2015) 1187–1192.

[11] J.Y. Sun, X.H. Zhao, W.R.K. Illeperuma, O. Chaudhuri, K.H. Oh, D.J. Mooney, et al., Highly stretchable and tough hydrogels, Nature 489 (7414) (2012) 133–136.

[12] T. Sakai, T. Matsunaga, Y. Yamamoto, C. Ito, R. Yoshida, S. Suzuki, et al., Design and fabrication of a high-strength hydrogel with ideally homogeneous network structure from tetrahedron-like macromonomers, Macromolecules 41 (14) (2008) 5379–5384.

[13] K. Mayumi, K. Ito, Structure and dynamics of polyrotaxane and slide-ring materials, Polymer 51 (20) (2010) 4461.

[14] D.C. Tuncaboylu, M. Sari, W. Oppermann, O. Okay, Tough and self-healing hydrogels formed via hydrophobic interactions, Macromolecules 44 (12) (2011) 4997–5005.

[15] E.A. Appel, M.W. Tibbitt, M.J. Webber, B.A. Mattix, O. Veiseh, R. Langer, Self-assembled hydrogels utilizing polymer-nanoparticle interactions, Nat. Commun. 6 (2015).

[16] B. Sharma, S. Fermanian, M. Gibson, S. Unterman, D.A. Herzka, B. Cascio, et al., Human cartilage repair with a photoreactive adhesive-hydrogel composite, Sci. Transl. Med. 5 (167) (2013), 167ra6.

[17] M.R. Prausnitz, R. Langer, Transdermal drug delivery, Nat. Biotechnol. 26 (11) (2008) 1261–1268.

[18] G. Cynthia, C. Kristie, K. Re, N. Ara, W. Gm, A dendritic thioester hydrogel based on thiol–thioester exchange as a dissolvable sealant system for wound closure, Angew. Chem. Int. Ed. 52 (52) (2013) 14070–14074.

[19] R. Feiner, L. Engel, S. Fleischer, M. Malki, I. Gal, A. Shapira, et al., Engineered hybrid cardiac patches with multifunctional electronics for online monitoring and regulation of tissue function, Nat. Mater. 15 (6) (2016) 679–685.

[20] L. Han, L. Yan, M. Wang, K. Wang, L. Fang, J. Zhou, et al., Transparent, adhesive, and conductive hydrogel for soft bioelectronics based on light-transmitting polydopamine-doped polypyrrole nanofibrils, Chem. Mater. 30 (16) (2018) 5561–5572.

[21] J.D. Kretlow, L. Klouda, A.G. Mikos, Injectable matrices and scaffolds for drug delivery in tissue engineering, Adv. Drug Deliv. Rev. 59 (4–5) (2007) 263–273.

[22] H. Park, J.S. Temenoff, T.A. Holland, Y. Tabata, A.G. Mikos, Delivery of TGF-beta1 and chondrocytes via injectable, biodegradable hydrogels for cartilage tissue engineering applications, Biomaterials 26 (34) (2005) 7095–7103.

[23] J.Y. Lai, Y.T. Li, Functional assessment of cross-linked porous gelatin hydrogels for bioengineered cell sheet carriers, Biomacromolecules 11 (5) (2010) 1387–1397.

[24] T. Mimura, S. Amano, S. Yokoo, S. Uchida, S. Yamagami, T. Usui, et al., Tissue engineering of corneal stroma with rabbit fibroblast precursors and gelatin hydrogels, Mol. Vis. 14 (2008) 1819–1828.

[25] J.Y. Lai, Y.T. Li, C.H. Cho, T.C. Yu, Nanoscale modification of porous gelatin scaffolds with chondroitin sulfate for corneal stromal tissue engineering, Int. J. Nanomed. 7 (2012) 1101–1114.

[26] M.G. Haugh, M.J. Jaasma, F.J. O'Brien, The effect of dehydrothermal treatment on the mechanical and structural properties of collagen-GAG scaffolds, J. Biomed. Mater. Res. 89 (2) (2009) 363–369. Epub 2008/04/24.

[27] K. Yue, G. Trujillo-de Santiago, M.M. Alvarez, A. Tamayol, N. Annabi, A. Khademhosseini, Synthesis, properties, and biomedical applications of gelatin methacryloyl (GelMA) hydrogels, Biomaterials 73 (2015) 254–271.

[28] X. Zhao, Q. Lang, L. Yildirimer, Z.Y. Lin, W. Cui, N. Annabi, et al., Photocrosslinkable gelatin hydrogel for epidermal tissue engineering, Adv Healthc Mater 5 (1) (2016) 108–118.

[29] M. Rafat, F. Li, P. Fagerholm, N.S. Lagali, M.A. Watsky, R. Munger, et al., PEG-stabilized carbodiimide crosslinked collagen–chitosan hydrogels for corneal tissue engineering, Biomaterials 29 (29) (2008) 3960–3972.

[30] E. Shirzaei Sani, A. Kheirkhah, D. Rana, Z. Sun, W. Foulsham, A. Sheikhi, et al., Sutureless repair of corneal injuries using naturally derived bioadhesive hydrogels, Sci. Adv. 5 (3) (2019), eaav1281.

[31] J.W. Nichol, S.T. Koshy, H. Bae, C.M. Hwang, S. Yamanlar, A. Khademhosseini, Cell-laden microengineered gelatin methacrylate hydrogels, Biomaterials 31 (21) (2010) 5536–5544.

[32] A. Nagai, J.B. Miller, P. Kos, S. Elkassih, H. Xiong, D.J. Siegwart, Tumor imaging based on photon upconversion of Pt(II) porphyrin rhodamine Co-modified NIR excitable cellulose enhanced by aggregation, ACS Biomater. Sci. Eng. 1 (12) (2015) 1206–1210.

[33] Y.-C. Chen, R.-Z. Lin, H. Qi, Y. Yang, H. Bae, J.M. Melero-Martin, et al., Functional human vascular network generated in photocrosslinkable gelatin methacrylate hydrogels, Adv. Funct. Mater. 22 (10) (2012) 2027–2039.

[34] S. Sharifi, H. Sharifi, C. Guild, M.M. Islam, K.D. Tran, C. Patzer, et al., Toward electron-beam sterilization of a pre-assembled Boston keratoprosthesis, Ocul. Surf. 20 (2021) 176–184.

[35] Sharifi S, Islam MM, Sharifi H, Islam R, Huq TN, Nilsson PH, et al. Electron beam sterilization of poly(methyl methacrylate)—physicochemical and biological aspects. Macromol. Biosci..n/a(n/a):2000379.

[36] S. Sharifi, M.M. Islam, H. Sharifi, R. Islam, P.H. Nilsson, C.H. Dohlman, et al., Sputter deposition of titanium on poly(methyl methacrylate) enhances corneal biocompatibility, Transl. Vision Sci. Technol. 9 (13) (2020) 41.

[37] L.B. Koh, M.M. Islam, D. Mitra, C.W. Noel, K. Merrett, S. Odorcic, et al., Epoxy cross-linked collagen and collagen-laminin Peptide hydrogels as corneal substitutes, J. Funct. Biomater. 4 (3) (2013) 162–177. Epub 2013/01/01.

[38] J.M. Hackett, C. Ferguson, E. Dare, C.R. McLaughlin, M. Griffith, Optimal neural differentiation and extension of hybrid neuroblastoma cells (NDC) for nerve-target evaluations using a multifactorial approach, Toxicol. Vitro 24 (2) (2010) 567–577.

[39] R. Sharifi, S. Mahmoudzadeh, M.M. Islam, D. Koza, C.H. Dohlman, J. Chodosh, et al., Covalent functionalization of pmma surface with l-3,4-dihydroxyphenylalanine (L-DOPA) to enhance its biocompatibility and adhesion to corneal tissue, Adv Mater Interfaces 7 (2020), 1900767.

[40] P. Seifert, Modified Hiraoka TEM grid staining apparatus and technique using 3D printed materials and gadolinium triacetate tetrahydrate, a nonradioactive uranyl acetate substitute, J. Histotechnol. 40 (4) (2017) 130–135.
[41] T.E. Mollnes, O.L. Brekke, M. Fung, H. Fure, D. Christiansen, G. Bergseth, et al., Essential role of the C5a receptor in E coli-induced oxidative burst and phagocytosis revealed by a novel lepirudin-based human whole blood model of inflammation, Blood 100 (5) (2002) 1869–1877. Epub 2002/08/15.
[42] G. Bergseth, J.K. Ludviksen, M. Kirschfink, P.C. Giclas, B. Nilsson, T.E. Mollnes, An international serum standard for application in assays to detect human complement activation products, Molecular immunology 56 (3) (2013) 232–239.
[43] K.-H. Chen, D. Azar, N.C. Joyce, Transplantation of adult human corneal endothelium ex vivo: a morphologic study, Cornea 20 (7) (2001).
[44] M. Gonzalez-Andrades, R. Sharifi, M.M. Islam, T. Divoux, M. Haist, E.I. Paschalis, et al., Improving the practicality and safety of artificial corneas: pre-assembly and gamma-rays sterilization of the Boston Keratoprosthesis, Ocul. Surf. 16 (3) (2018) 322–330.
[45] H. Garoff, W. Ansorge, Improvements of DNA sequencing gels, Anal. Biochem. 115 (2) (1981) 450–457.
[46] E. Hoch, C. Schuh, T. Hirth, G.E. Tovar, K. Borchers, Stiff gelatin hydrogels can be photo-chemically synthesized from low viscous gelatin solutions using molecularly functionalized gelatin with a high degree of methacrylation, J. Mater. Sci. Mater. Med. 23 (11) (2012) 2607–2617.
[47] P.N. Shah, N. Kim, Z. Huang, M. Jayamanna, A. Kokil, A. Pine, et al., Environmentally benign synthesis of vinyl ester resin from biowaste glycerin, RSC Adv. 5 (48) (2015) 38673–38679.
[48] I. Noshadi, S. Hong, K.E. Sullivan, E. Shirzaei Sani, R. Portillo-Lara, A. Tamayol, et al., In vitro and in vivo analysis of visible light crosslinkable gelatin methacryloyl (GelMA) hydrogels, Biomater. Sci. 5 (10) (2017) 2093–2105.
[49] C.S. Bahney, T.J. Lujan, C.W. Hsu, M. Bottlang, J.L. West, B. Johnstone, Visible light photoinitiation of mesenchymal stem cell-laden bioresponsive hydrogels, Eur. Cell. Mater. 22 (2011) 43–55.
[50] ASTM D638-14, Standard Test Method for Tensile Properties of Plastics, ASTM International, West Conshohocken, PA, 2014.
[51] H. Suo, D. Zhang, J. Yin, J. Qian, Z.L. Wu, J. Fu, Interpenetrating polymer network hydrogels composed of chitosan and photocrosslinkable gelatin with enhanced mechanical properties for tissue engineering, Mater. Sci. Eng. C 92 (2018) 612–620.
[52] A. Assmann, A. Vegh, M. Ghasemi-Rad, S. Bagherifard, G. Cheng, E.S. Sani, et al., A highly adhesive and naturally derived sealant, Biomaterials 140 (2017) 115–127.
[53] A. Katchalsky, S. Lifson, H. Exsenberg, Equation of swelling for polyelectrolyte gels, J. Polym. Sci. 7 (5) (1951) 571–574.
[54] H.B. Bohidar, S.S. Jena, Kinetics of sol–gel transition in thermoreversible gelation of gelatin, J. Chem. Phys. 98 (11) (1993) 8970–8977.
[55] M.M. Islam, R. Sharifi, M. Gonzalez-Andrades, Corneal tissue engineering, in: J. L. Alió, J.L. Alió del Barrio, F. Arnalich-Montiel (Eds.), Corneal Regeneration : Therapy and Surgery, Springer International Publishing, Cham, 2019, pp. 23–37.
[56] R. Sharifi, Y. Yang, Y. Adibnia, C.H. Dohlman, J. Chodosh, M. Gonzalez-Andrades, Finding an optimal corneal xenograft using comparative analysis of corneal matrix proteins across species, Sci Rep-Uk. 9 (1) (2019) 1876.
[57] C. Engler, C. Kelliher, C.L. Speck, A.S. Jun, Assessment of attachment factors for primary cultured human corneal endothelial cells, Cornea 28 (9) (2009) 1050–1054. Epub 2009/09/03.
[58] P.W. Madden, J.N. Lai, K.A. George, T. Giovenco, D.G. Harkin, T.V. Chirila, Human corneal endothelial cell growth on a silk fibroin membrane, Biomaterials 32 (17) (2011) 4076–4084. Epub 2011/03/24.
[59] L.B. Koh, M.M. Islam, D. Mitra, C.W. Noel, K. Merrett, S. Odorcic, et al., Epoxy cross-linked collagen and collagen-laminin Peptide hydrogels as corneal substitutes, J. Funct. Biomater. 4 (3) (2013) 162–177.
[60] D. Li, J. Zhou, F. Chowdhury, J. Cheng, N. Wang, F. Wang, Role of mechanical factors in fate decisions of stem cells, Regen. Med. 6 (2) (2011) 229–240.
[61] G.M. Cruise, D.S. Scharp, J.A. Hubbell, Characterization of permeability and network structure of interfacially photopolymerized poly(ethylene glycol) diacrylate hydrogels, Biomaterials 19 (14) (1998) 1287–1294. Epub 1998/08/28.
[62] A. Hoshikawa, Y. Nakayama, T. Matsuda, H. Oda, K. Nakamura, K. Mabuchi, Encapsulation of chondrocytes in photopolymerizable styrenated gelatin for cartilage tissue engineering, Tissue Eng. 12 (8) (2006) 2333–2341. Epub 2006/09/14.
[63] L. Almany, D. Seliktar, Biosynthetic hydrogel scaffolds made from fibrinogen and polyethylene glycol for 3D cell cultures, Biomaterials 26 (15) (2005) 2467–2477. Epub 2004/12/09.
[64] S.J. Bryant, K.S. Anseth, Controlling the spatial distribution of ECM components in degradable PEG hydrogels for tissue engineering cartilage, J. Biomed. Mater. Res. 64 (1) (2003) 70–79. Epub 2002/12/17.
[65] D.S. Benoit, A.R. Durney, K.S. Anseth, Manipulations in hydrogel degradation behavior enhance osteoblast function and mineralized tissue formation, Tissue Eng. 12 (6) (2006) 1663–1673. Epub 2006/07/19.
[66] F. Tabatabaei, K. Moharamzadeh, L. Tayebi, Fibroblast encapsulation in gelatin methacryloyl (GelMA) versus collagen hydrogel as substrates for oral mucosa tissue engineering, J Oral Biol Craniofac Res 10 (4) (2020) 573–577. Epub 2020/09/18.
[67] L. Li, C. Lu, L. Wang, M. Chen, J. White, X. Hao, et al., Gelatin-based photocurable hydrogels for corneal wound repair, ACS Appl. Mater. Interfaces 10 (16) (2018) 13283–13292. Epub 2018/04/06.
[68] J.K. Kutty, E. Cho, J. Soo Lee, N.R. Vyavahare, K. Webb, The effect of hyaluronic acid incorporation on fibroblast spreading and proliferation within PEG-diacrylate based semi-interpenetrating networks, Biomaterials 28 (33) (2007) 4928–4938. Epub 2007/08/28.
[69] I. Garzon, M.A. Martin-Piedra, C. Alfonso-Rodriguez, M. Gonzalez-Andrades, V. Carriel, C. Martinez-Gomez, et al., Generation of a biomimetic human artificial cornea model using Wharton's jelly mesenchymal stem cells, Invest. Ophthalmol. Vis. Sci. 55 (7) (2014) 4073–4083. Epub 2014/06/08.
[70] M.M. Islam, R. Sharifi, S. Mamodaly, R. Islam, D. Nahra, D.B. Abusamra, et al., Effects of gamma radiation sterilization on the structural and biological properties of decellularized corneal xenografts, Acta Biomater. 96 (2019) 330–344. Epub 2019/07/10.
[71] M. Gonzalez-Andrades, J. de la Cruz Cardona, A.M. Ionescu, A. Campos, M. Del Mar Perez, M. Alaminos, Generation of bioengineered corneas with decellularized xenografts and human keratocytes, Invest. Ophthalmol. Vis. Sci. 52 (1) (2011) 215–222. Epub 2010/08/27.
[72] M. Alaminos, M. Gonzalez-Andrades, J.I. Munoz-Avila, I. Garzon, M.C. Sanchez-Quevedo, A. Campos, Volumetric and ionic regulation during the in vitro development of a corneal endothelial barrier, Exp. Eye Res. 86 (5) (2008) 758–769. Epub 2008/04/04.
[73] T.E. Mollnes, Complement and biocompatibility, Vox Sang. 74 (Suppl 2) (1998) 303–307. Epub 1998/08/15.
[74] Y. Modinger, G.Q. Teixeira, C. Neidlinger-Wilke, A. Ignatius, Role of the complement system in the response to orthopedic biomaterials, Int. J. Mol. Sci. 19 (11) (2018). Epub 2018/10/31.
[75] S.S. Bhatia, Ocular surface sealants and adhesives, Ocul. Surf. 4 (3) (2006) 146–154.
[76] G. Trujillo-de Santiago, R. Sharifi, K. Yue, E.S. Sani, S.S. Kashaf, M.M. Alvarez, et al., Ocular adhesives: design, chemistry, crosslinking mechanisms, and applications, Biomaterials 197 (2019) 345–367.
[77] Jhanji V, Young AL, Mehta JS, Sharma N, Agarwal T, Vajpayee RB. Management of corneal perforation. Surv. Ophthalmol..56(6):522-538.
[78] Food and Drug Administration, ReSure® Sealant - P130004, 2014.
[79] A. Sharma, R. Kaur, S. Kumar, P. Gupta, S. Pandav, B. Patnaik, et al., Fibrin glue versus N-butyl-2-cyanoacrylate in corneal perforations, Ophthalmology 110 (2) (2003) 291–298.
[80] C. Kilic Bektas, V. Hasirci, Mimicking corneal stroma using keratocyte-loaded photopolymerizable methacrylated gelatin hydrogels, J. Tissue Eng. Regenerative Med. 12 (4) (2018) e1899–e1910.
[81] K.A. Vakalopoulos, Z.Q. Wu, L. Kroese, G.J. Kleinrensink, J. Jeekel, R. Vendamme, et al., Mechanical strength and rheological properties of tissue adhesives with regard to colorectal anastomosis an ex vivo study, Ann. Surg. 261 (2) (2015) 323–331.
[82] M. Ravi, V. Paramesh, S.R. Kaviya, E. Anuradha, F.D. Solomon, 3D cell culture systems: advantages and applications, J. Cell. Physiol. 230 (1) (2015) 16–26.